

Metasurfaces and Metamaterials for Electromagnetics

A. Alù, *Fellow, IEEE*, S. Maci, *Fellow, IEEE*, N. Engheta, *Life Fellow, IEEE*

Abstract—Metamaterials (MTMs) and metasurfaces (MTSs) are engineered materials and surfaces constituted by a distribution of electrically small particles that collectively exhibit emerging properties that enable superior control over the electromagnetic field. This paper reviews various electromagnetics research areas relevant to the antennas and propagation community impacted by MTMs and MTSs, including extreme material responses, space and surface wave control, electromagnetic manipulation in space and time, nonlocal responses, hyperbolic phenomena, near-zero permittivity, nonreciprocal and nonlinear effects, and topological metasurfaces. Modeling, design, characterization, and applications of these devices are discussed, as well as their impact on antenna and electromagnetic engineering.

Index Terms—Metasurfaces, metamaterials, electromagnetics, antennas, wave control.

I. INTRODUCTION

Metamaterials (MTMs) have been dominating the research scene in electromagnetics (EM), antennas and propagation, revolutionizing designs and enabling unprecedented functionalities. They are providing significant impact across a variety of fields and applications. In optics, MTMs have enabled invisibility cloaks, superlenses and extreme control over light propagation. In acoustics, they enable the manipulation of sound waves for applications such as noise reduction, soundproofing and medical imaging. Their ability to control electromagnetic waves with precision has opened new frontiers in enhancing antenna performance, miniaturization and beamforming capabilities, energy harvesting and wireless power transfer systems. In healthcare, MTMs play a role in imaging technologies, biosensors, and even therapeutic devices. Their applications also extend to structural engineering, where they are used to create materials with tailored mechanical properties, and in quantum technologies, where they contribute to photonic devices and quantum communications. Metasurfaces (MTSs) [1], [2], [3], [4], [5], [6], emerged as a powerful extension of MTMs in this technological trajectory, offering a planarized platform especially important at microwave frequencies, reducing the dimensionality, significantly simplifying design and

A. Alù is with CUNY Advanced Science Research Center. N. Engheta is with Department of Electrical and Systems Engineering, University of Pennsylvania, and S. Maci is with the Department of Information Engineering and Mathematics, University of Siena (e-mails: aalu@gc.cuny.edu, engheta@seas.upenn.edu macis@dii.unisi.it.) A.A., N.E. were supported by the Air Force Office of Scientific Research (AFOSR) MURI program grant FA9550-21-1-0312, the AFOSR grant FA9550-23-1-0307 and the Simons Foundation. S.M. was supported by the European Space Agency (ESA-ESTEC, The Netherlands) by the Italian Ministry of the Research through a Project of relevant Italian Interest (PRIN), and by the Italian National Recovery and Resilience Plan (NRRP) of Next Generation EU, partnership on “Telecommunications of the Future” (PE0000001 - program “RESTART”).

fabrication. Comprised of patterned subwavelength elements on a thin planar substrate, metasurfaces enable precise control over wavefronts, including phase, amplitude, and polarization. This 2D approach not only addressed the limitations of bulk MTMs but also unlocked new possibilities for ultra-compact and highly efficient devices. While artificial materials have trace back to 1898 with the work of J. C. Bose [7], the seminal work of Pendry in 1999 [8] marked a turning point for this research field, as he demonstrated that subwavelength metallic structures could exhibit an effective negative refractive index, previously thought to be unattainable with conventional materials. This was associated with the possibility to make a perfect lens [9]. The term itself “metamaterial” originated from the work of R. M. Walser [10], in the context of extreme magnetism in artificial materials, but has since then assumed a much broader meaning. The term, derived from the Greek prefix ‘meta-’ meaning ‘beyond,’ reflects the transformative nature of these materials; it defines structures, engineered to exhibit EM properties not found in nature. The years 2000-2010, MTMs and MTSs were designed with uniform periodic arrangements of elements; the emphasis was given in those years to double-negative (DNG) materials, backward-wave transmission lines, which mimic DNG responses [11], and perfect lenses, a canonical application of DNG materials and a holy grail of the early days of metamaterials. Epsilon-near-zero (ENZ) materials soon emerged as another exciting platform leveraging extreme forms of EM material response, well suited to realize plasmonic cloaking [12] and optical nanocircuits [13], developed in those years. In the same period MTS research was put forward, even if the term was not in use yet. Several new concepts and applications in microwaves and antennas were born, such as artificial magnetic surfaces and bandgaps for surface waves, concepts leading to several applications, such as reduction of surface wave coupling in antenna arrays, improvement of planar-antenna efficiency, quasi-TEM propagation waveguides, miniaturized cavity resonators, enhancing bandwidth of small antennas, flat absorbers. In a second generation, MTSs were designed to adiabatically change constitutive parameters or boundary conditions. The first hint was given in the context of transformation optics [14], envisioning the possibility of realizing a perfect EM cloak [15]. The adiabatic modulation of constitutive parameters was exploited in MTSs to design metalenses, MTS antennas, meta-deflectors and meta-radomes, near-field focusing and hyperbolic MTS. Today, we are facing a transition to a third generation (3G) of MTM/SS, where MTSs change boundary conditions in space and time, becoming controllable and intelligent. MTSs reconfigurability can be achieved by using

electronics, time-varying materials, or multiple switchable feed-points distributed over the MTS. Reconfigurable ultra-thin surfaces can be designed to be capable of dynamically transforming impinging wavefronts in response to changes in the environment, hold promise for the development of smart environment [16], [17], [18]. Time-varying elements have also the potential to overcome fundamental limitations of passive metastructures, such as reciprocity constraints and passivity. Recent investigations have explored time-varying MTS and nonlinear MTS for their nonreciprocal properties, which do not require the presence of external magnets to break time-reversal symmetry [19]. Active MTSs offer the possibility to transcend the bandwidth limitations inherent in passive structures, achieving non Foster dispersion [20]. However, challenges persist concerning the stability of these components and the difficulty in attaining sufficient gain at high frequencies. Given the breadth of applications and of research breakthroughs enabled by MTMs, the selection of topics presented in this paper is a personal view of the authors to highlight a few relevant and remarkable advances that may be of appeal to the broad community of antenna and propagation engineers.

II. EPSILON-NEAR-ZERO (ENZ) METAMATERIALS AND NEAR ZERO INDEX (NZI) PHOTONICS

One of the interesting and impactful categories of metamaterials is those in which the real part of the relative permittivity (or relative permeability) attains values near zero around certain operating frequencies [21], [22], [23] [24]. These media, which we refer to as epsilon-near-zero (ENZ) and mu-near-zero (MNZ) media, exhibit relatively low refractive index. Consequently, in such structures, the waves experience “stretched” wavelengths at the operating frequencies, leading to numerous fascinating and exciting wave phenomena that form the foundations of the field of near-zero-index (NZI) electromagnetics and photonics. Some of these features are briefly summarized below. For further details, the reader is referred to various review articles in the literature [25], [26], [27], [28].

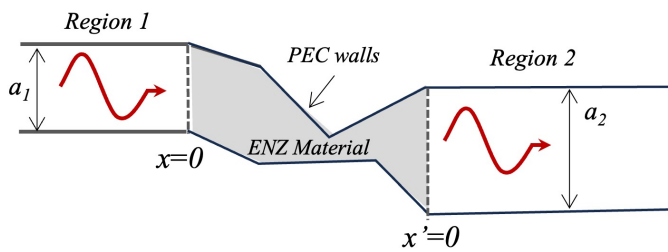


Fig. 1. ENZ-based Supercoupling: Geometry of the two-dimensional problem in which two parallel-plate waveguides with PEC connected via a transition PEC waveguide, filled with an ENZ material. Adapted with permission from [23], copyright © American Physical Society.

A. ENZ Supercoupling

One of the exciting features exhibited in ENZ media is the phenomenon of “supercoupling”, which was discovered

in 2006 [23]. Consider the two-dimensional problem of two parallel-plate waveguides made of perfect electric conducting (PEC) walls arbitrarily positioned next to each other and connected via a transition waveguide section also made of PEC with a narrow (but arbitrarily long) passage. (See Fig. 1). The incident wave inside the first waveguide is a TEM mode travelling towards the second waveguide. It is obvious that if the material inside of this waveguide structure is made of a conventional dielectric (e.g., air), the incident wave may experience a noticeable reflection since the waveguide has an abrupt change in its geometrical cross-section. However, when the transition region is filled with an ENZ material, it was shown analytically in [23] that the reflection coefficient for this TEM mode is given by $\Gamma = \frac{(a_1-a_2)+ik_o\mu_r A_D}{(a_1+a_2)-ik_o\mu_r A_D}$ where the parameters are described below. In order to bring the reflection coefficient to zero, one needs to choose the waveguide heights $a_1 = a_2$, implying that the two waveguides should have the same height and, moreover, have one of the three parameters k_0 , μ_r , and A_D be zero. Of these three, making $k_0 = \omega/c$ to be zero results in $\omega = 0$, indicating a DC voltage, which is not of interest here. Another possibility is to require $\mu_r \approx 0$, but this would mean that the material in the transition region should also be an MNZ (in addition to being ENZ, i.e., it should be epsilon-and-mu-near-zero (EMNZ)) medium, which is not preferable due to its complexity.) And yet another possibility is to make A_D , which is the cross-sectional area of the ENZ region, to be near zero. This latter case is the most interesting one, demonstrating a highly unusual and counter-intuitive phenomenon, which we coined “supercoupling” [23], [29]. When the transition region is filled with a material with the Drude dispersion, the reflection coefficient approaches zero at the plasma frequency of the Drude material at the limit of very low loss. It is interesting to note that as we make the cross section area of the transition region smaller and smaller (i.e., A_D gets smaller and smaller), the wave tunnels through the region better and better, which is rather counterintuitive. We have experimentally verified this phenomenon in various waveguide scenarios [30], [31], as shown in Fig. 2.

Some of the examples of ENZ materials include transparent conducting oxides (TCO), such as indium tin oxide (ITO) in the near-IR regime , silicon carbide (SiC) in mid IR wavelength [32], and some topological insulators in the UV regime [33]. If one would like to have the ENZ materials at other desired frequencies, one can engineer metamaterial structures that exhibit some of the ENZ properties. For example, at the microwave frequencies, metallic rectangular waveguides operating at the TE10 cut-off frequency exhibit wave properties resembling some of the near-zero-index features . Moreover, photonic crystals with the Dirac dispersion with accidental degeneracy also possess an effective refractive index near zero, which can be used as NZI platforms at optical frequencies [34], [35].

B. Photonic Doping

Another fascinating property of ENZ structures is the phenomenon of ENZ-based “Photonic Doping”, which was introduced and developed in 2017 [36]. Inspired by the notion

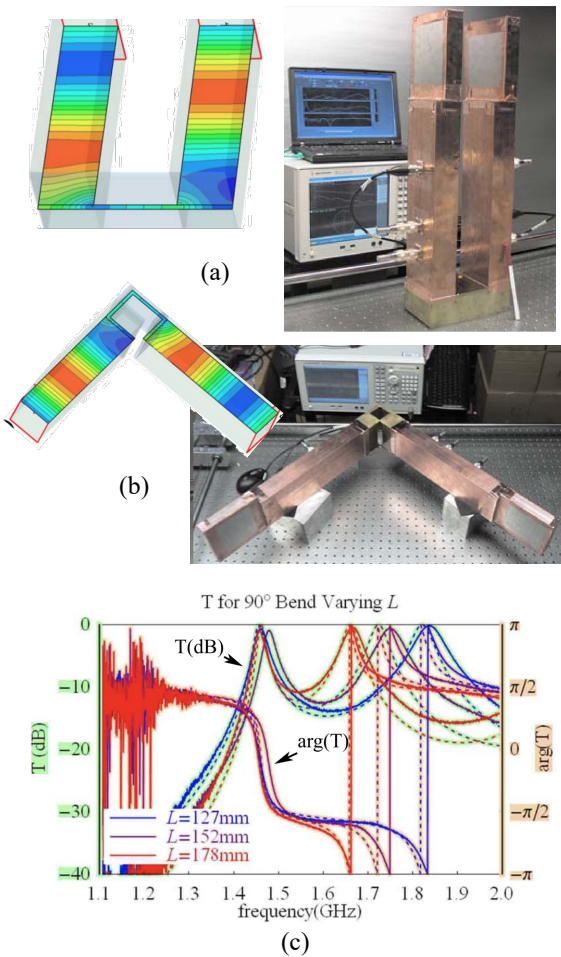


Fig. 2. Experimental verification of ENZ-based Supercoupling. Geometry of the experimental setup for the waveguide: (a) 180° bend; (b) 90° bend. (c) Amplitude and phase of the transmission coefficient for different length of the ENZ channel. At the ENZ frequency (which is equivalent to the cut-off frequency of the narrow channel), the transmission coefficient has maximum magnitude and zero phase. Adapted with permission from [31], copyright © American Institute of Physics

of electronic doping, which is the foundation behind semiconductor science and technology, we asked the following question: *Can we have photonic doping?* It is well known that in wave interaction with photonic crystals operating within their band gap, the presence of a defect can affect this interaction, allowing the propagation of new modes. *But what about creating a “defect” by adding a “photonic dopant” within an ENZ medium?* This led to an interesting phenomenon, which we called ENZ-based photonic doping.

Consider a two-dimensional column of a lossless ENZ material with an arbitrary cross-sectional shape (See Fig. 3a). An incident electromagnetic TM wave illuminates this column, resulting in scattered fields inside and outside the column. Now, we insert another column of material made of conventional dielectric material, with another arbitrary cross-section smaller than the ENZ cross-section. The addition of this dielectric rod certainly affects and changes the scattered fields inside and outside. The question is: *For the outside observer, can this dielectric-doped ENZ column be represented*

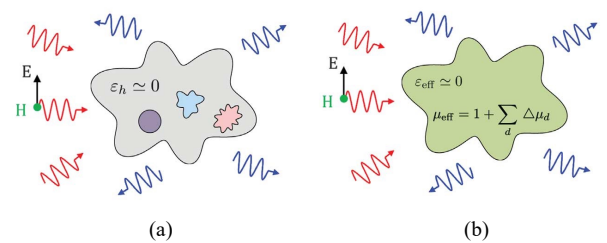


Fig. 3. ENZ-based Photonic Doping: (a) Schematic of a two-dimensional (2D) ENZ nonmagnetic host column ($\epsilon_h \approx 0$) with several nonmagnetic dielectric rod dopants. (b) Equivalent homogeneous 2D structure (as seen by an outside observer) with the same cross-sectional shape and size, exhibiting relative permittivity $\epsilon_{eff} \approx 0$ and effective relative permeability $\mu_{eff} = 1 + \sum_d \Delta\mu_d$. (Adapted with permission from [36], copyright © American Association for the Advancement of Science.)

by homogenized effective medium parameters? In other words, can we assign an effective permittivity and an effective permeability to this doped ENZ structure? In [36], we offered a comprehensive answer to these questions and demonstrated the results theoretically and experimentally. It turned out that starting with an ENZ column in which relative permittivity is zero (because this is ENZ) and relative permeability is unity (because the ENZ column is non-magnetic), adding the dielectric rod with conventional dielectric constant different from zero and non-magnetic unity relative permeability within this ENZ column leads to a new structure in which the effective relative permittivity of the entire structure still stays at zero, but its effective relative permeability is different from unity (Fig. 3b). The photonic doping contribution, denoted as $\Delta\mu_d$ quantifies the perturbation (as viewed by an outside observer) to the effective magnetic response of the composite system due to each dopant. Remarkably, while the effective relative permittivity of the structure remains near zero (i.e., $\epsilon_{eff} \approx 0$), the effective relative permeability becomes a tailorable parameter, described as $\mu_{eff} = 1 + \sum_d \Delta\mu_d$ where each term $\Delta\mu_d$ represents the individual contribution of a photonic dopant to the magnetic permeability of the ENZ-dielectric composite. This contribution arises from the change in the magnetic flux induced by the dielectric dopant and is dependent on the cross-sectional shape, size and the constitutive parameters of the dopant, and the overall area of the ENZ host, while it is independent of the location of the dopant (as long as it is within the ENZ host) and the cross-sectional shape of the external geometry of the ENZ host. It is also important to point out that, in the limit of an ideal lossless ENZ host, each $\Delta\mu_d$ is independent of the interaction among the dopants and their locations. This effective permeability engineering enables the realization of novel “single-inclusion” metamaterials with exotic magnetic responses—including negative, high, or near-zero effective permeability—using nonmagnetic constituents. While this is rather counterintuitive, it is an excellent example of a metamaterial in which a combination of two non-magnetic materials (one being a simple dielectric rod and another being an ENZ column) leads to a composite structure in which the effective permittivity remains at zero value, but the effective permeability can be engineered to be different from the permeability of each of the constituents,

effectively providing “single-inclusion metamaterials” (Fig.3). This allows us to engineer metamaterials with unconventional values for effective permeability such as negative μ , near-zero μ , high positive μ , etc. It is also relevant to mention another interesting feature of NZI photonics exhibited in the cavity resonators made of ENZ materials.

Another intriguing aspect is introduced next. It is well known that in conventional cavity resonators, the resonance frequency is closely dependent on the shape of the cavity. However, cavities made of ENZ materials may reduce or eliminate this dependence of the resonance frequency on the external shape. Instead, the resonance frequency may be “locked” to the ENZ frequency and be effectively independent of the external shape [37], [38].

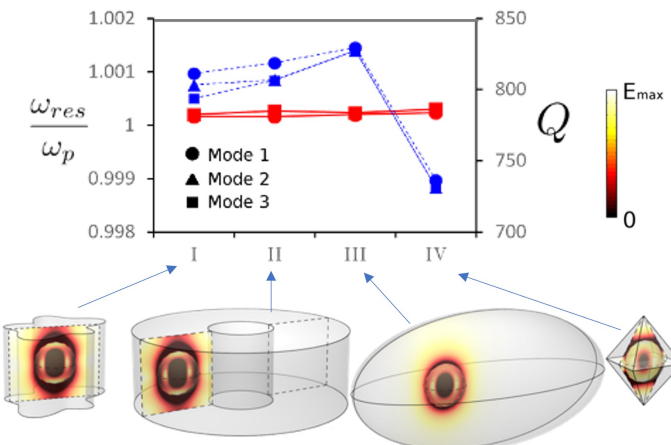


Fig. 4. Four cavities with arbitrary shapes made of ENZ materials, doped with a dielectric sphere, exhibit the same resonance frequency but different quality factor (Q). The same dielectric sphere is used as the dopant in all configurations, allowing consistent comparison of the resulting electromagnetic response. Adapted with permission from [26], copyright © Optical Society of America.

Figure 4 presents this feature with reference to four open cavities. These cavities, with different arbitrary shapes, are all assumed to be made of ENZ material, with a dielectric sphere embedded in them as a photonic dopant. The numerical simulations show that the resonance frequencies of all these cavities are similar, and all are near the plasma frequency of the Drude material for ENZ, while their quality factors (Q) are different. This indeed exhibits how the resonance frequency is locked to the plasma (ENZ) frequency, independent of the shape of the cavity, while the Q of the cavity can be engineered by the shape of the cavity, which may offer interesting applications in flexible photonics and quantum optics [39]. We have experimentally verified both concepts of ENZ-based photonic doping and geometry-independent ENZ-based cavity [36]. As shown in Fig.5a, we built three cavity resonators with three different cross-sectional shapes (but the same cross-sectional areas), with a single dielectric rod inserted in them as a dopant. This dielectric dopant can be placed in three different locations in each of the three cavities. We performed transmission experiments in these three cavities (each with three different locations of the dielectric rod), and the results are presented in Fig. 5b. All nine cases exhibit the same resonance frequencies

but different Q values, verifying both phenomena of photonic doping and geometry-independent cavity features.

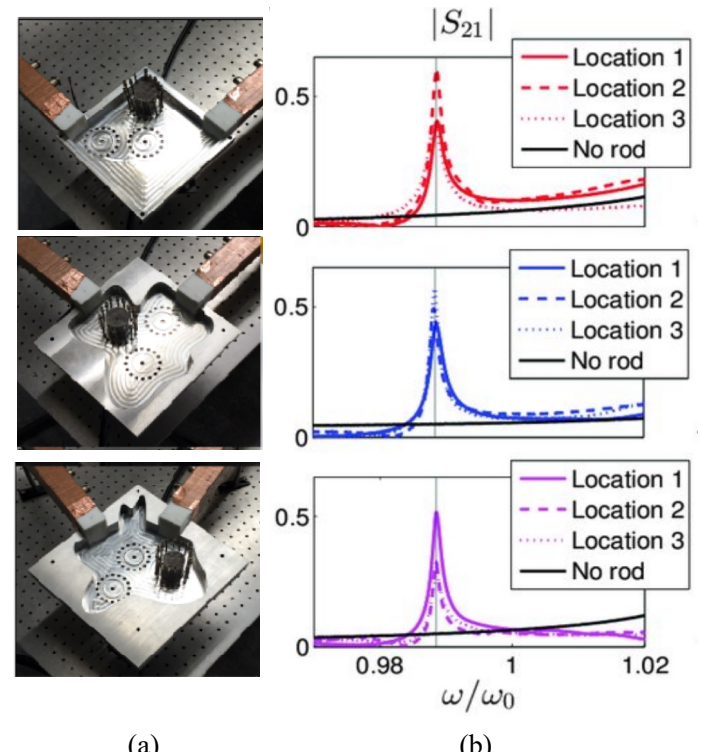


Fig. 5. Experimental verification of ENZ-based photonic doping and geometry-independent cavity: (a) Three different metallic cavities with arbitrary cross-sectional shapes (but the same cross-sectional areas), doped with a dielectric rod that is placed at three different locations in each cavity. (b) Amplitude of the transmission coefficients at the waveguide ports for the three cavities in the three different positions. All nine cases show the same resonance transmission. Adapted with permission from [36], copyright © American Association for the Advancement of Science.

C. Other relevant wave physics phenomena

The ENZ, MNZ, and EMNZ materials, forming the bases of the NZI photonics and electromagnetics, offer numerous unique and exciting phenomena have been discussed above, but many more exist, which are summarized next. Extended Purcell effects in nanophotonics [40], enhanced nonlinearity [41], [42], [43], [44], topologically protected photonic states [45], beyond-diffraction-limit imaging in the far-field, [46], classic analogue of Meissner effect and levitation for electric field near an ENZ surface [47], [48], plasmonic cloaking and transparency [12], ENZ-based quantum optics [39], in which the EMNZ materials can in principle reduce or even theoretically inhibit vacuum fluctuations, and therefore can profoundly affect the spontaneous emission of an excited atom, leading to engineering of the vacuum Rabi oscillation using strong coupling of an excited atom with zero-index cavity without detuning the cavity, ENZ-based thermal radiation engineering [49], [50] in which the ENZ object can control the direction of thermal radiation somewhat analogous to partially spatially coherent phased arrays, and more. It has also been shown that optical flow in near-zero-index media behave very

similarly to the ideal fluid in fluid dynamics, thus ushering a new phenomenon of *fluidic electrodynamics* [51], which shortly after was experimentally verified in the microwave domain [52].

III. SPACE/SURFACE WAVE CONTROL WITH MTS

MTSs can be categorized by their interaction mechanisms with waves and designed for three purposes (Fig. 6): i) achieving unusual reflection/transmission properties of space waves [53], [54], [55], [56], [57] (Fig. 6 2a-b), ii) modifying the dispersion of surface wave for obtaining flat lenses or metasurface antennas. The first category enables non-specular reflective surfaces (Fig. 6a), where output beams are redirected by modifying the MTS's linear phase. MTS lenses (Fig. 6b) act as optical lenses, readdressing rays from the feed. Flat Optical lenses (Fig. 6c) operate modifying the local dispersion; surface wave (SW) antennas (Fig. 6d) use in-plane monopole feeds to excite cylindrical SWs. Challenges include canceling specular reflections in (a)-(b) and efficiently exciting SWs while controlling leakage attenuation along their path in (c). In (d), periodic boundary condition (BC) modulations transform SWs into curvilinear leaky waves (LWs), creating a radiating apertures with amplitude control achieved through 2D attenuation distribution design.

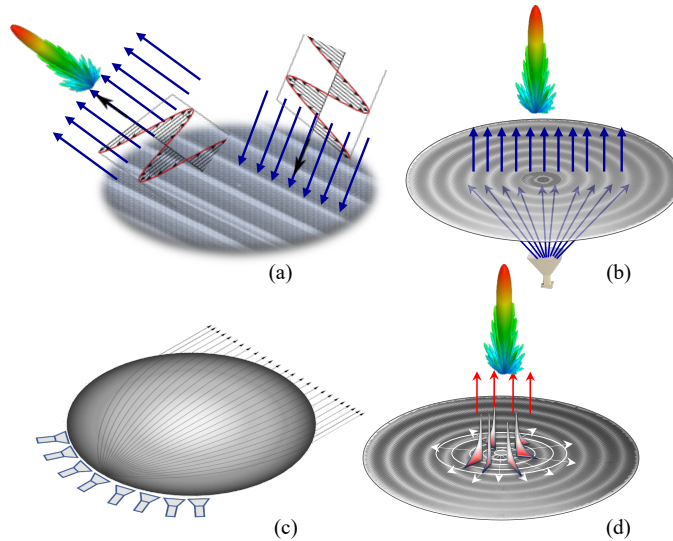


Fig. 6. Different types of MTS; (a) passive Reflective Intelligent Surfaces (RIS); (b) MTS Lens, (c) flat metasurface lens (d) MTS antenna based on surface-to-leaky wave transformation.

A. Phase-gradient metasurfaces

Phase-gradient metasurfaces, initially introduced by the Capasso group [58], are a class of two-dimensional engineered structures designed to manipulate electromagnetic waves through subwavelength-scale spatial modulation of their optical properties. The term "gradient" here specifically refers to the spatial variation of the local phase response imparted by the metasurface. While this subsection focuses on phase-gradient implementations, spatial modulation remains a common design principle across all metasurface types discussed in

this section, irrespective of the underlying physical mechanism (e.g., geometric phase, nonlocality, or time modulation). Pioneering work on this subject was also developed by the group of Shalaev [59]. By introducing abrupt phase shifts across the surface, gradient metasurfaces control wavefronts with high precision, enabling functionalities like beam steering, focusing, and holography. These devices achieve their effects by tailoring the geometry and arrangement of subwavelength scatterers to induce desired phase, amplitude, and polarization transformations, bypassing the need for bulky refractive elements. Gradient metasurfaces implement the generalized Snell's law of reflection and refraction, $\frac{\partial \Phi_{\text{trans}}}{\partial(k_s)} = \sin \theta_{\text{trans}} - \sin \theta_{\text{inc}}$, where the phase gradient of the transmission coefficient (first member) across the surface alters the traditional wavefront propagation rules readdressing the ray from an angle θ_{inc} to an angle θ_{trans} wrt the local surface normal. This allows light to bend at arbitrary angles, independent of the material's intrinsic properties, and enables compact, flat optical devices like metalenses, where the required phase profile to focus light is encoded directly into the metasurface, eliminating the need for bulky curved lenses. An expression equivalent to the gradient of the transmission phase can be also used for readdressing the reflection through a gradient of the *reflection coefficient phase*. One significant challenge in the design of gradient multi-metasurfaces, particularly for microwave applications, is achieving impedance matching to minimize reflections. To overcome this impairment, Huygens-type metasurfaces have become a preferred solution.

B. Huygens MTS and Bianisotropic BC

By carefully balancing electric and magnetic dipole moments, Huygens metasurfaces (HMS) can completely suppress reflections and ensure efficient energy transfer across the surface. These MTS were inspired by the Huygens' principle, or its vector form known as the Love Equivalence Principle. HMS are transparent MTS that can transform the wavefront of the incident space-wave field to a prescribed transmitted wave. Thin lenses, beam deflectors, beam splitters, polarizers and multifunctional devices can be realized using HMSs. HMS implement through MTS the equivalence theorem in a generalized Physical Optics (PO) framework, in contrast to the GO framework of gradient MTS presented [58]. HMS can be achieved playing with electric dipoles and electric loops located in a plane orthogonal to the MTS plane. To achieve the desired unidirectional scattering, HMS particles must support balanced symmetric and antisymmetric current modes with respect to the plane of the MTS. When excited by an incident wave, the symmetric current flow generates an equivalent electric dipole, while the antisymmetric current produces an orthogonal magnetic dipole. By adjusting the relative excitation of these modes through meta-atom geometry, the magnitudes of the electric and magnetic current components can be controlled, creating the necessary electromagnetic field discontinuity in accordance with the equivalence principle [60]. The interaction of these currents with the electromagnetic fields at the metasurface boundary leads to bianisotropic tensor-impedance boundary conditions.

This concept was developed by the groups of S. Tretyakov, A. Grbic and C. Caloz [2], [61], [62], [63], [64]. The design of an MTS lens is achieved by considering the meta-atoms as immersed in a periodic environment and manipulating the phase of the transmission coefficients. The variation in transmission phase among adjacent elements creates the local gradient necessary for beam shaping. In [65], it has been shown that the optimization of the Floquet coefficient in a mode matching type reiterarted analysis can get a more general solution that can also control the bandwidth. Although the natural application of HMS is for lenses and focusing antenna system, other uses in the antenna domain are illustrated in Fig. 7. These include increasing the scan range in phased arrays [66], [67] while mitigating the scan blindness effect (7a), creating a virtual corrugated horn using a dual metasurface (7c), and potentially tilting the beam of a horn for integration into a reflector antenna multifocal system for beam shaping from the GEO-orbit satellite (Fig. 7d).

An important extension to conventional gradient metasurface designs involves the realization of *achromatic metasurfaces*, which are capable of maintaining a constant group delay across a broad frequency band. Unlike standard phase-gradient metasurfaces that typically operate under monochromatic or narrowband conditions, achromatic designs enable pulse-preserving functionalities such as broadband beam steering and focusing. These characteristics make them particularly attractive for dispersion engineering and wideband antenna applications, including their use as compact, planar analogues of parabolic reflectors. Broadband achromatic focusing based on refractive index gradients was demonstrated in [68], and large-angle, multifunctional metagratings utilizing freeform multimode geometries were reported in [69].

C. Pancharatnam-Berry phase MTSs

The Pancharatnam-phase, is a geometrical phase that arises when a system undergoes a cyclic adiabatic evolution in its parameter space. It is particularly relevant in optics, where it is associated with the manipulation of the polarization state of light. The phenomenon was discovered by S. Pancharatnam in 1956 [70] in optics and generalized by M. Berry in 1984 [71] to any adiabatic evolution of Hamiltonian in quantum mechanics. In optics and EM, this property provides a way to create circularly polarized lenses (PBL) or deflector (PBD), namely half-wave thick plate that converts an RCP incident ray in a LCP transmitted ray which also cumulate a geometrical phase (PB-phase), that can be controlled to focus or deflect beams. This phenomenon is well devised in optical components (see [72] and references therein). It can be used for creating deflectors (Fig. 7d), and antennas (Fig. 11).

D. Anomalous Reflection and RIS

The next generation of wireless communications (6G) needs a new architectural platform not only for transmission/reception, but also for sensing, communication, computing and, above all, an environment that can be cooperative and programmable; this visionary concept is denoted as Smart Radio Environment (SRE). The key technology

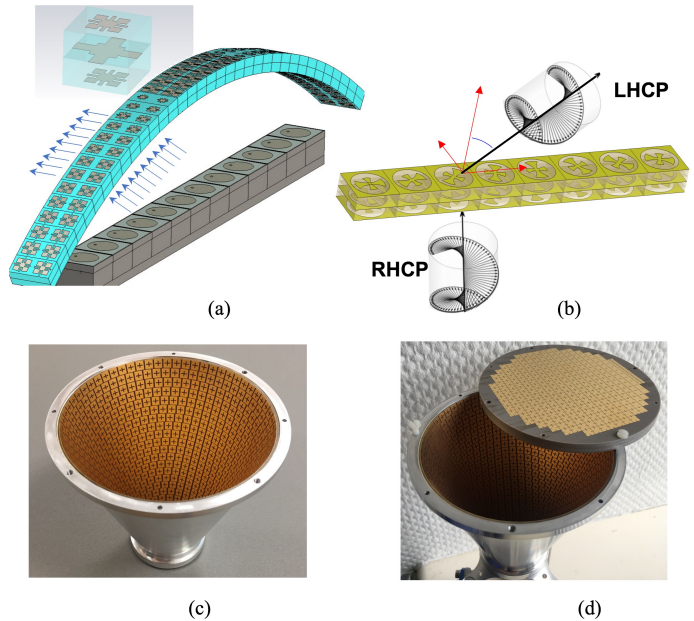


Fig. 7. Example of MTS for space wave control in transmission; (a) HMS based on a three-layer planar elements for increasing scan angle in phased array; (b) Pancharatnam-Berry screen with polarization inversion and phase gradient; (c) metasurface horn equivalent to a corrugated horn (adapted from [73], copyright IEEE); (d) Horn with a HSM top cover lens for beam deflection [74].

underpinning SREs is represented by metasurfaces (MTSs) of next generation, which can be denoted with the general acronym of RISs (Reconfigurable Intelligent Surfaces [75], [76]. Controlling reflection is, in some respects, simpler than controlling transmission because the current and fields are confined to the same side of the structure, which simplifies the boundary conditions. However, this approach offers fewer degrees of freedom to effectively cancel the specular reflection. According to the local approach, the impedance profile of an anomalous reflector is designed to provide a reflection phase linearly varying to compensate the phase mismatch between the incident and reflected waves, assuming that the local reflection coefficient is the same of the corresponding homogeneous MTS.

A milestone in the development of intelligent and programmable metasurfaces was the introduction of multi-layer architectures for routing control signals beneath the reflective backplane. This approach enables the independent addressing and actuation of metasurface elements while maintaining compactness and reflective functionality. One of the earliest implementations of such a concept was demonstrated by Chen and Tretyakov [77], who proposed a three-layer intelligent metasurface system for routing electronic control signals to unit cells. This design was further extended by Zhou *et al.* [78], who realized a programmable metasurface with embedded multi-layer circuitry, allowing complex wavefront manipulation and adaptive functionalities in real-time. These works represent foundational contributions to the field and illustrate a key technological pathway for enabling reconfigurability in large-scale metasurface systems.

E. Nonlocal MTS

The common design principles to design metasurfaces described in the previous sections follow a local approach: they neglect in first approximation the coupling between closely spaced unit elements, and tailor them independently to manipulate pixel by pixel the incoming wavefront. While this approach has been offering a powerful playground for wavefront control, these local MTSs face fundamental constraints in their operation, in particular in terms of efficiency and chromatic aberrations, which stem from symmetry and passivity constraints. Over the years, several of these bounds have been unveiled [79], indicating that the compactification of optical devices can come at a price.

An interesting knob to fight some of these challenges consists in empowering the coupling among elements, and engineer the nonlocality of the MTS response. We call these surfaces nonlocal, since they rely on the long-range interactions of the constituent elements. Metagratings [80], [81], are an early example of such structures: by leveraging periodic structures, like gratings, but tailoring the unit cell in nontrivial ways to engage the lattice resonance, it is possible to realize extreme control over the EM wavefront, for instance supporting near-grazing beam steering with unitary efficiency. These structures rely on long-range resonances stemming from their periodicity. These principles can be further empowered by introducing tailored perturbations, which break periodicity but preserve the lattice resonances. The response of nonlocal metasurfaces combines the advantages of local responses with spatially-extended resonances from meta-gratings, offering new degrees of freedom to pattern the incoming EM wavefront, both spatially and spectrally [82]. Nonlocal metasurfaces have been opening new opportunities for wavefront manipulation, including wavefront selectivity, [83] and multi-functionality [84]. Emerging applications of nonlocal metasurfaces beyond wavefront control include the possibility of filtering and processing images in momentum space, realizing analog-based computers, which we feature in more detail in Section VIII. [85], [86], [87], [88], [89], [90]. Tailored nonlocalities can also impart spatial and temporal coherence to random material processes, enabling a new form of control over thermal emission and photoluminescence. Using such metasurfaces it is possible to heat up a surface in order to efficiently emit tailored wavefronts with desired amplitude, phase and polarization, [91], [92], integrating the source itself inside the metasurface design.

F. Graphene-based Metasurfaces

Graphene and related 2D materials are enabling platforms for tunable metasurfaces, particularly in the terahertz and mid-infrared regimes. Their atomically thin structure and gate-tunable conductivity support strong subwavelength plasmon confinement and dynamic wave control. Foundational models based on dyadic Green's functions have been developed to characterize graphene surface waves [93], while nonlocal effects—relevant at large in-plane wavevectors—have been shown to induce spatial dispersion and novel responses [94]. Beyond conventional tuning, graphene's electrostatic control

over chemical potential allows realization of transformation-optical devices on a single layer. Vakil and Engheta demonstrated how spatial modulation of conductivity enables wave steering, beam shaping, and ultrathin optical elements [95]. These principles underpin recent advances in reconfigurable, low-profile photonic circuits based on 2D-material metasurfaces.

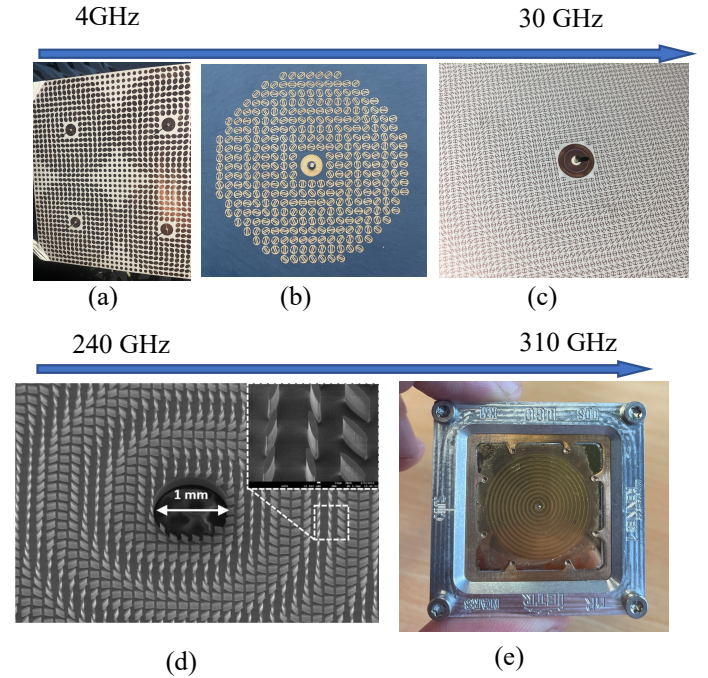


Fig. 8. Realizations of MTS antennas at various frequencies, from 4 GHz to mm waves in PCB and only metal technology (courtesy of UltiMetas, (J. Chazelas, C. Triponez, Canseliet (a), Wave-Up (F. Caminita, C. Della Giovampaola, G. Minatti) (b), (c), IETR (D. Gonzalez-Ovejero) (d), (e)

G. Metasurface antennas

Metasurface antennas are examples of non-local surface-wave control, in which the BC are used to transform the surface wave in a leaky-wave. Analytical models of leaky-wave structures, play an essential role in designing these antennas, [96], that emerged in the last years as a promising platform for next generation planar devices in a broad range of frequencies, [97], [98], [99] [100], [101] especially for space applications. In particular, in the microwave range this solution is characterized by low-cost, lightweight, and simple integration with electronic circuits, since MTSs can be realized in PCB technology by printing electrically small patches over a dielectric slab. MTS antennas can be applied in a range of frequency from 4 GHz to 30 GHz in PCB technology, and from 30GHz to 340 GHz in only metal technology (see Figure 8) [102]. In PCB technology, various type of printed elements can be used [103], each one with a proper peculiarity in terms of bandwidth and polarization control.

The basic structure (Fig.9) consists on a single-feed monopole with a circular patch on top, that launch a cylindrical wavefront surface wave over the texture structure, with

efficiency of SW power till 80%, which is macro-modulated by using the elements. The modulation interact with the surface wave and produces a shaped beam [104], [105]. The surface texture may also control near field and multifunctionality [106]. The MTS behavior can then be conveniently described in terms of homogenized boundary (BC) conditions of impedance type. At a difference with respect to the MTS for space wave control, the BC are studied as a support of surface wave, exploring their *dispersion properties* in terms of transverse resonance condition. With sub-wavelength unit cells, MTSs can use homogenized impedance boundary conditions, linking average electric and magnetic field tangential components and enable a very fast Method of Moment analysis, like the one presented in [107]. This approach eliminates the need for detailed modeling of individual elements, significantly lowering computational demands and preventing numerical issues. The effective BCs at each unit cell rely on local periodicity, assuming a micro-periodic environment defined by the subwavelength period of small elements, unlike the macro-period of global modulation (see left inset of Fig. 9).

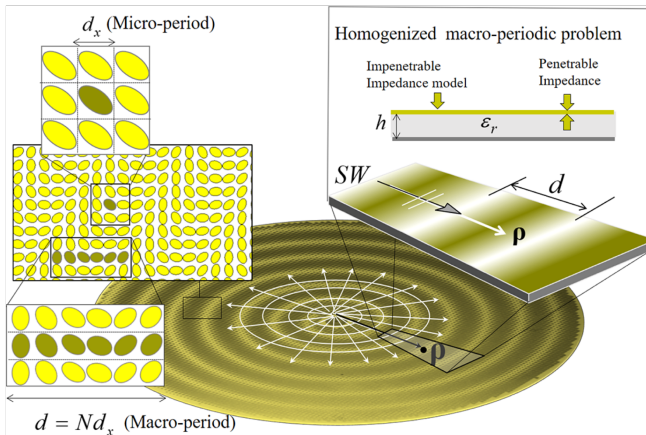


Fig. 9. Metasurface antenna and illustration of the double-scale periodicity (left hand zoom) and of the homogenized impedance models (right hand side zoom, top). The local problem for the extraction of the nonlocal parameters is shows in the right hand side zoom, bottom

For MTSs constituted by only metal pins, BCs are expressed via an “impenetrable” tensor impedance linking tangential electric and magnetic fields $\mathbf{E}_t^+ = \underline{\underline{Z}} \cdot \hat{\mathbf{z}} \times \mathbf{H}_t^+$. For microwave and millimeter-wave MTSs, losses are negligible, making the impedance tensor anti-Hermitian. This model is realistic for weak k -dispersivity. This doesn’t happen for MTSs constituted by metallic-patch on grounded slabs, which are better modeled with “penetrable” impedance BCs, relating tangential electric and magnetic field discontinuities $\mathbf{E}_t = \underline{\underline{Z}}_s \hat{\mathbf{z}} \times [\mathbf{H}_t^+ - \mathbf{H}_t^-]$. The latter model extends to multilayer environments with interlayer interactions captured via multiport networks, excluding Floquet modes attenuated in neighboring layers [108]. We note that even if many authors continue to use the impenetrable impedance model, for printed patch MTS, the penetrable model is much more accurate, since incorporate the effect of space dispersivity by the grounded slab Green’s function [109]. Like in space-type MTS, the analysis of the interac-

tion of an electromagnetic plane wave with a periodically modulated MTS antenna is based on a local unidirectional-gradient homogenized surface impedance which matches the local boundary conditions even with curvilinear modulation. This unidirectional-gradient, macro-periodic impedance problem represents therefore the “canonical” problem for the MTS design. The synthesis of these antennas play therefore with a dual scale. the periodicity of the impedance profile (macro-periodicity d), as opposed to the micro-periodicity d_0 related to the subwavelength unit cell used for the MTS implementations. The macro-periodicity account for the non-locality of the EM interaction. An approach for a rigorous solution of the problem, which can be seen as a generalization of [110], is proposed in [111]. In PCB-based MTSs, modulation is achieved by varying patch size, shape, or orientation across adjacent unit cells, employing a local micro-periodicity approximation. Unit cells are analyzed in periodic environments to construct impedance databases based on geometric parameters or tunable material states. This yields continuous or discrete impedance maps, enabling MTS synthesis by selecting elements that best fit the target impedance. For anisotropic tensor impedance, synthesis involves least-square minimization across all tensor components.

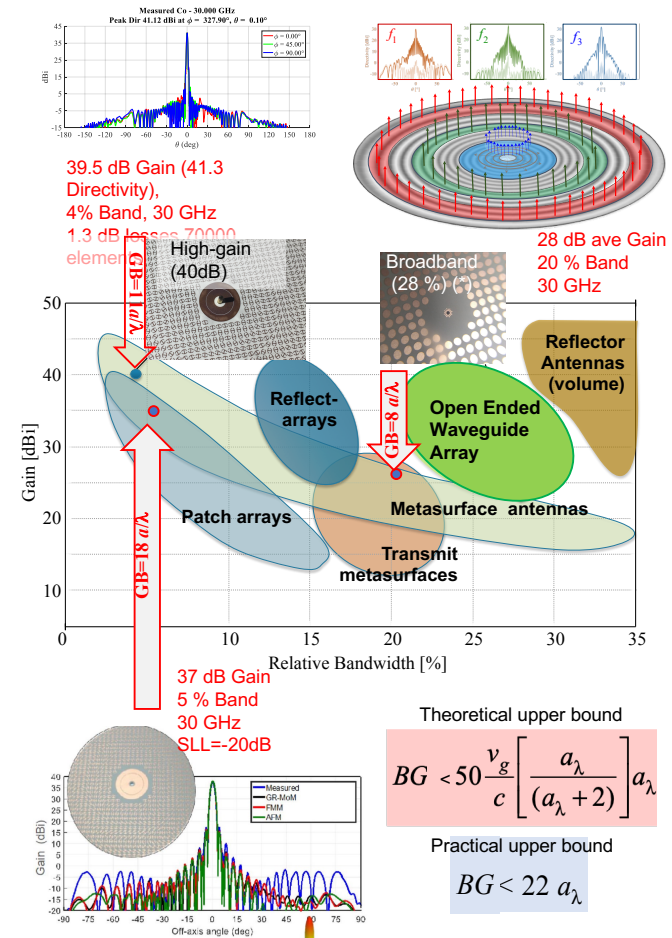


Fig. 10. Range of product bandwidth-gain and theoretical bounds of MTS antennas. The inset shows three antenna prototypes and their collocation in terms of product bandwidth gain

Fig. 10 illustrates the range of bandwidth and gain covered by different metasurface antenna configurations. It compares metasurface antennas to other antenna types, such as reflector antennas, patch arrays, and open-ended waveguides, in terms of relative percent bandwidth and gain (dBi). The plot highlights how metasurface antennas effectively bridge the gap between traditional high-gain quasi optical system and planar patch array antennas. The theoretical constraints on the gain-bandwidth product (GB) are also emphasized in the figure, indicating the upper limits for metasurface antennas in practical applications [112], [113], [114].

H. Hyperbolic MTSs

One of the most extreme forms of EM wave control supported by MTMs and MTSs consists in hyperbolic surface wave propagation, which is associated with highly confined and directional waves that defy the limitations commonly introduced by diffraction. MTMs and MTSs supporting hyperbolic surface waves enable extreme wave confinement over broad bandwidths and enhanced forms of light-matter interactions. The surface wave dispersion supported by these structures is characterized by hyperbolic iso-frequency contours (IFCs) [115], [116], which have a different topology compared to conventional IFCs of waveguide or surface wave modes. In particular, the open nature of hyperbolic IFCs implies access to very large momenta, and hence very large field confinement and very strong local density of states for antennas or emitters placed close to the surface. This phenomenon is not narrowband but can happen over very broad bandwidths. Hyperbolic wave propagation was first demonstrated in hyperbolic MTMs, which provide similar features but for space waves. The advantage of hyperbolic metasurfaces is that the fields are not limited to live inside the material, but they are confined to the surface, being therefore accessible and suffering reduced losses. Hyperbolic surfaces have been applied to control the Coulomb force between atoms, enhancing electromagnetic interactions, wave trapping, chemical sensing and Purcell enhancement [117], [118], [119], [120], [121], [122], [123], [124]. This response can be achieved by tailoring the effective surface conductivity tensor $\underline{\sigma} = \sigma_{xx}\hat{x}\hat{x} + \sigma_{xy}\hat{x}\hat{y} + \sigma_{yx}\hat{y}\hat{x} + \sigma_{yy}\hat{y}\hat{y}$ in such a way that $\text{Im}\{\sigma_{xx}\} \text{Im}\{\sigma_{yy}\}$ where Im denotes the imaginary part. Physically, such surfaces support capacitive/inductive responses for orthogonal polarizations of the electric field. This extreme anisotropy can be induced for instance with a dense grid mesh [125]. At higher frequencies, arrays of resonant meta-atoms with large anisotropic response can be used, and even some natural materials feature hyperbolic responses, both in the bulk and at their interface with air, due to the large anisotropy of their material resonances. While hyperbolic metasurfaces offer the potential to support high-momentum surface waves due to their extreme anisotropy, physical constraints limit the maximum achievable wavevector. Factors such as material losses, spatial dispersion (nonlocal effects), and fabrication limitations restrict the confinement and propagation of ultra-high-k modes [126] [121]. These considerations are essential for evaluating practical perfor-

mance in sensing, sub-diffraction imaging, and waveguiding applications.

The application of hyperbolic MTS from antennas [127] to surface wave control and light emission patterning, enhancement and routing, has become prominent in the literature, and holds the promise to an exciting future for this research area. Broken symmetries introduced in these responses may further enhance directionality, field confinement and bandwidth of operation [128], [129]. Double polarization control of a hyperbolic MTS can be achieved by alternating strips with dual impedance boundary conditions, which can be realized, for instance, using complementary slots and dipoles. This type of MTS exhibits hyperbolicity across all frequencies with TE-TM degeneracy and demonstrates super-canalization at the frequency singularities of the dual strips [130].

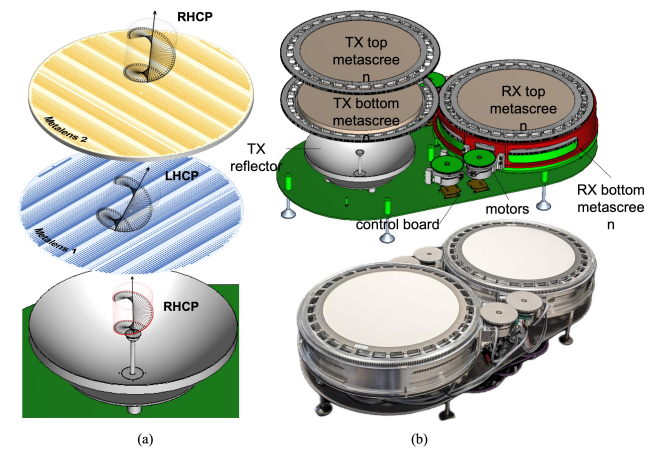


Fig. 11. Microwave Risley Lens by using Pancharatnam-Berry screens fed by a short focal reflector. Realization by Wave-Up srl (Siena, Italy).

IV. RECONFIGURABILITY BY MTS

A. Aperture sharing: Port Multiplexing

A major practical goal for wireless networks is to obtain multiple directive beams from a single aperture simultaneously. For MTS antennas, this aperture sharing concept foresees, in essence, the superposition of two or more modulation functions point by point on the entire aperture. The basic concept was developed in [131] by using a reactance modulation tensor in a form of a summation of modulation function, that is eventually implemented by printed elements. Assigning one feed-point per beam instead of a single, unique feed, allows for multiplexing by a simple switching network. One could consider dividing the aperture in distinct angular sectors, each excited by a different source. This approach requires a feed network scheme in which each source illuminates only its corresponding sector. Consequently, the overall system is more complex in comparison to the single feed version. Nevertheless, one can still apply the superposition of the modulation patterns to obtain one independent beam per source. A practical example is given in [132] where seven ports are obtained by superimposing 7 different modulation [132]. A radar monopulse application is shown in [133].

B. Beam scanning by rotations: microwave Risley lenses

The first proposed scanning antenna solution for the low-profile ground user terminal is based on Rotating Metalenses (RMSA). Each antenna (Rx and TX) is constituted by a fixed primary antenna (PA) with broadside pencil beam and two parallel Metalenses that can be rotated independently around the axis of the primary radiator. A schematic representation of the RMSA is shown in Fig. 12. The principle of operation of such architecture is based on the use of Pantcharatnam-Berry metaleenses which are designed to realize a double deflection of the incident wave (see Fig. 7a). The Metaleenses can be considered a planar version of the so-called optical Risley prisms [134], where beam steering both in azimuth and elevation is obtained by using a couple of rotatable dielectric wedges located in front of a fixed primary antenna. The role of the prisms is to provide a desired variable phase shift to the impinging wave. The RMSA are an effective alternative implementation of the dielectric wedges to obtain a compact and lightweight design, with low reflection losses.

C. Beam scanning by switching: Reflecting Luneburg Lenses

Beam scanning by switching can be obtained by the use of a Reflecting Luneburg Lense (RLL). RLL introduced in [135], is a type of beam-former, which consists of two vertically stacked parallel plate waveguides (PPWs) of circular shape. The bottom PPW is filled with a graded index (GRIN) medium with azimuthal symmetry, which addresses the rays launched by a point source along curvilinear paths up to a corner reflector. Upon encountering this reflecting boundary, the rays emerge collimated in the top PPW. Owing to the lens' symmetry, one can generate plane waves with arbitrary directions by just switching the azimuthal position of the point source in the bottom layer. Fig.12(a)-(c) shows the operational principle. The RLL has been implemented using bed of nails with higher symmetries [136], offering the advantage of a large bandwidth. Integration with transverse stubs has been recently proposed for obtaining a wide-angle scanning [137].

D. Electronic reconfigurability

Fast reconfigurability of the beam and beam scanning based on dynamic, electronically reconfigurable MTSs are the most impactful challenges for MTS. This can be achieved through the inclusion in the MTS of active devices or tunable materials; this way, the electric features of the inclusions become voltage controlled, and, hence, the boundary conditions offered by the MTS can be properly adjusted by an external control. Although this concept has been already demonstrated [138], [139] existing solutions still need to be improved in terms of efficiency. In fact, active devices and tunable materials yield an increase of the antenna losses, with a consequent reduction of gain and increase of power demand; losses become more important when working at higher frequencies (e.g. Ka-band). The use of micromechanical systems or piezoelectric devices have been proposed, but they may suffer of low reliability and an MTS antenna based on such devices may be too sensitive to the external vibrations if installed on moving vehicles. Beam

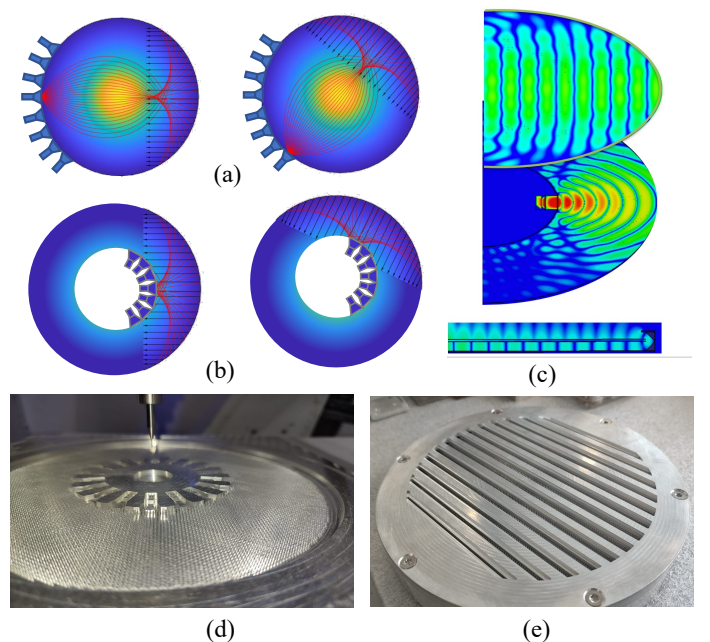


Fig. 12. Reflecting Luneburg Lens (RLL). (a) peripheral feeding (the rays exhibit turning points). (b) Internal feeding; (c) Screen shot of the field on top and lower floor; (d) realization of the bottom floor by bed of nails (e); realization of the top floor by transverse stubs (d,e, Adaptation from [137], copyright IEEE)

scanning in surface-wave-based reconfigurable MTS antennas can be obtained through two different approaches. The first one is based on the control of the SW wavenumber; the second one on the control of the periodicity. Both allow for a 1D scanning of the radiated beam. In particular, the first approach may allow beam scanning at fixed frequency with a single voltage control. A theoretical analysis is available [140] using liquid crystals as tunable substrate. The radiating part is constituted by a parallel plate waveguide partially filled by liquid crystals with gradually modulated, electrically small slots etched on the upper wall. Commercial products based on similar concept are available from Kymeta corporation (<https://www.kymetacorp.com/>). In addition to liquid crystals, tunable materials for MTS include ferroelectric and phase-changing materials, such as vanadium dioxide. Advances in phase changing materials would bring a significant benefit to reconfigurable MTSs, in terms of losses and switching time reduction, as well as increase of temperature stability. The second approach is based on the tuning of the modulation period, and therefore it requires multiple control signals across the MTS. As a difference with the previous approach, these controls can also be binary. If all the MTS unit cells are individually piloted, 2D scanning can be also achieved through the pointwise control of the MTS modulation. This strategy was applied and experimentally validated in [141] to implement elevation scanning in an array of modulated MTS channels for RIS in 5G scenarios. In that case, the pointing angle was precisely controlled by piloting a network of PIN diodes connected to metallic dipoles printed on top of a PCB. MTS with integrated active devices, instead of

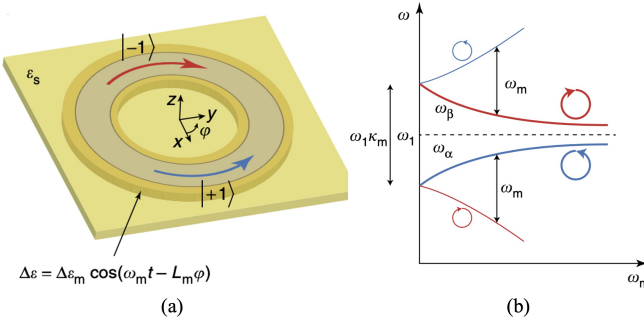


Fig. 13. (a) Azimuthally symmetric ring resonator with a spatiotemporal modulation of permittivity. The modulation follows the form of an azimuthally propagating wave in the $\pm\phi$ direction. In the absence of modulation, the resonator supports two degenerate counter-propagating states. (b) Sub-state eigenfrequencies versus the modulation frequency. Adaptation from [144], copyright Springer Nature.

discrete ones, would bring advantages in terms of reliability, losses, and performances. In this framework, the power consumption for the control network can be decreased by using field effect transistors instead of pin diodes as switches. However, realizing integrated devices on a wide area requires significant improvement of the accuracy and repeatability of the fabrication processes.

V. NONRECIPROCAL MTMs

Nonreciprocity implies broken symmetry in transmission, a fundamental property for many EM devices, i.e., isolators, circulators and gyrators. These devices and their operations are crucial in communications, signal processing and all-optical computing. Yet, nonreciprocity typically requires an external bias, impeding integration and compact footprints [142]. The most common approach to break reciprocity indeed relies on magnetic bias and magneto-optical phenomena, but the integration of magnets and materials supporting these responses into compact devices is very challenging. Time modulation schemes offer an exciting platform to break this constraint, i.e., enable magnet-free nonreciprocal devices, and MTMs have enabled their implementation in various forms and for a wide range of frequencies [143], [144], [145], [146], [19] [147] [148] [149].

By tailoring a MTM or a MTS to mechanically or synthetically rotate in time, through a time-varying modulation pattern that mimics a rotation, one can induce a form of artificial magnetic bias to the device, which breaks reciprocity. This is seen, for instance, in Fig. 13, which shows the unit cell of a MTS that is modulated in time with a signal that synthesizes a rotating pattern, as indicated in Fig. 13a. Such a modulation pattern breaks the degeneracy of resonances supported by the MTS, inducing a splitting very much analogous to the Zeeman splitting observed in magnetically biased resonators. Fig. 13b shows how, by controlling the amplitude and phase of the modulation scheme it is possible to control such splitting, which indicates broken time-reversal symmetry and magnet-free nonreciprocity. Over the years, several practical implementations have been demonstrated using this concept, finding insightful ways to enhance the bandwidth of operation, limiting the

required frequency of modulation and its amplitude, and minimizing the energy required to drive the modulation. As a result, the demonstrated devices appear to be competitive to replace conventional magnet-based nonreciprocal elements for various platforms. An appealing alternative consists in breaking reciprocity through nonlinearities. This approach enables a fully passive form of nonreciprocity, which is bias-free, as it has been recently demonstrated in integrated photonic and radio-frequency systems. Recently, this solution has been also extended to free-space MTS operation, using ultrathin metasurfaces with tailored nonlinearities [150]. A bias-free silicon metasurface featuring large free-space nonreciprocity at telecom wavelengths was recently demonstrated by combining thermo-optic nonlinearities, naturally available in amorphous silicon, with a MTS design featuring broken vertical symmetry. The MTS supports a resonant mode with tailored dispersion and, as the input power grows, third-order nonlinearities shift the sharp resonance by an amount proportional to the local field intensity. Due to the broken vertical symmetry, input waves from opposite directions induce different local field intensities, leading to a direction-dependent resonance shift. As a result, large transmission contrast can be achieved within a range of input power levels and frequencies. To implement this mechanism within realistic power levels for free-space operation, it is crucial to enhance and control the nonlinear response. To address this challenge, in-plane broken symmetry was introduced in the MTS design. Such in-plane asymmetry supports a bandwidth response that can be tailored by varying the width ratio. By simultaneously optimizing out-of-plane and in-plane broken symmetries, nonreciprocal transmission with on-demand performance metrics can be achieved, only limited by fundamental bounds associated with time-reversal symmetry [151]. This design principle can be extended to different frequency ranges, and to different power levels engaging metasurfaces with tailored nonlinearities [152].

VI. TOPOLOGICAL MTS AND PTD MTS

A. Topological MTS

Topological photonics [153] leverages global properties of the EM field in either the spatial or momentum domains to provide robustness to the resulting response of photonic systems, unaffected by perturbations and noise. The idea is that topological quantities, describing global features, are not affected by small variations, and hence responses that leverage these quantities are inherently robust. Topological concepts have been applied successfully to metasurfaces to demonstrate guided wave propagation that is robust against imperfections. The bulk-boundary correspondence, one of the cornerstones of topological photonics, in fact guarantees that a guided mode must be supported at the boundary between domains with different topological features. Hence, by realizing MTSs described by different topological quantities and realizing an interface between them, we are bound to realize interface waves that propagate at the boundary with robust features, resilient to defects and disorder [154], [155]. A rigorous classification of Chern-type photonic insulators, based on the Green function formalism, was proposed in [156].

In addition, topological features can occur in real space, also associated with robustness. For instance, phase singularities in the far-field response associated with topological quantities, yield robustness to disorder, which ensure a wider control over the wavefront [157] [158]. These topological singularities can be associated with exceptional points, which can be realized in MTMs and MTSs featuring elements with balanced loss and gain [159], [160]. MTSs realized following these principles offer unique opportunities for EM control, not only limited to wavefront manipulation but also for lasing and source generation [161].

B. Parity Time-reversal Duality (PTD) MTS

Recent studies have demonstrated that reciprocal structures with parity time-reversal duality (PTD) symmetry [162] can be used to achieve protected propagation similar to the one of topological MTS. Indeed, it was discovered that a guiding structure supports backscatter-immune propagation if its transverse cross-section contains an axis whose direction inversion provides dual boundary conditions (BC) with respect to the original BC. Such type of waveguide is referred to as PTD-symmetric, since it remains unchanged when subjected to the combination of parity (P), time-reversal (T), and duality (D) transformations. Significantly, this feature can be attained in passive, lossless, and reciprocal guiding structures, which provides significant simplification for practical implementation, as opposed to active or non-reciprocal alternatives. Exact solutions are available for a class of closed domain PTD waveguides [163] [164]. Experimental validation of the concept and microwave device based on this concept [165] have been recently published both in closed domain [166] [167] [168] and open domain [169]. A similar approach has been devised in [170] where a class of non-resonant, self-dual planar metastructures capable of protected energy transmission from one side to the other through arbitrarily narrow apertures.

VII. 4D METAMATERIALS

In his December 8, 2000, Nobel lecture, Herbert Kroemer, who received the Nobel prize in physics for his work on semiconductor heterostructures, stated that “the interface is the device” [171]. This is indeed also the case in electromagnetics and optics, where interfaces and inhomogeneities in material parameters, e.g., permittivities and refractive indices, can tailor and manipulate electromagnetic and optical waves and fields. In Maxwellian electrodynamics, the “space” and the “time” exhibit certain symmetry and duality. Although these variables are mathematically analogous in many aspects, their physical roles in wave-matter interaction naturally have certain differences. In electromagnetic and optical devices and components, one often uses spatial inhomogeneities to manipulate the light in order to achieve useful functionalities. Waveguides, lenses, and diffractive elements are examples of such material inhomogeneities in space. But by bringing the dimension of “time” into the material parameter variation, one can have more degrees of freedom to tailor the waves. Exploring such space-time analogy in “4D waves” in electromagnetic metamaterials provides exciting possibilities and new

functionalities in light-matter interaction. 4D metamaterials are wave-based, material-based platforms in which some of the material parameters can vary with time (i.e., temporal inhomogeneities) in addition to (or instead of) varying in space (i.e., spatial inhomogeneities). Such 4D sculpting of waves in these structures leads to exciting wave phenomena.

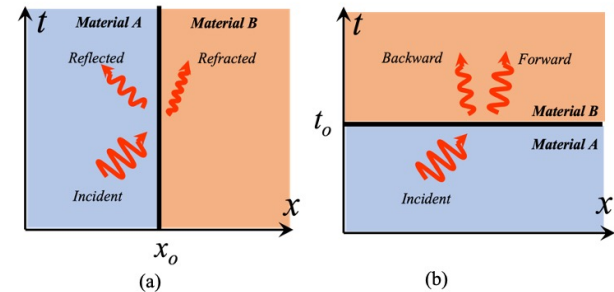


Fig. 14. Spatial and temporal interfaces: (a) two semi-infinite spatial media (Material A and Material B) have a common spatial interface at a given location in space (shown as x_0). (b) temporal interface occurs when Material A is changed to Material B at a given time (shown as t_0). Light interaction with such interfaces exhibits different features.

The study of time-dependent platforms has a long history dating back to 1950s [172], [173]. In 1958, Morgenthaler studied theoretically how the electromagnetic wave in a medium behaves when the phase velocity experiences rapid variation [174]. In 1971, Fante investigated the electromagnetic wave interaction with time-varying media with a spatial boundary [175]. Recently, many investigators all over the world have studied various aspects of spatiotemporal platforms [176], [177], [178], [179], [180], [181], [182], [183], [184], [185], [186]. In 4D metamaterials, we can have the concept of “time interface” (or ‘temporal interface’), which is the temporal analogue of the conventional “space interface” (or “spatial interface”). Just as the space interface is the interface/boundary between two media in space, a time interface is when a medium undergoes rapid change of its parameters in time. These two interfaces have certain similarities and differences. When an electromagnetic wave is incident at a spatial interface, the reflected and refracted waves have the same frequency (for linear media), but the refracted wave exhibits a different wavectors (See Fig 14a). So, in this case, the electromagnetic energy is conserved (assuming no loss in the media), but the electromagnetic momentum is changed. However, for the temporal interface, when the parameter (e.g., permittivity) of an unbounded medium is rapidly changed in time while the electromagnetic wave is in the medium, two waves, a forward (FW) wave and a backward (BW) wave, are generated. In this case, the electromagnetic momentum is conserved (i.e., the wave vector k is unchanged) while, in contrast, the frequency of the wave is modified. (See Fig 14b). The BW wave resulting from such a time interface has been exploited as a method for time reversal, e.g., in water waves [187]. The BW in the transmission line structure has been experimentally observed for the first time recently [188]. It is important to highlight the fact that the temporal interface must also obey the causality while breaking the time-reversal symmetry. There-

fore, such temporal interfaces and time-varying platforms can be utilized to achieve magnet-free nonreciprocity [189], [19]. They can also be used to explore and mimic some of the relativistic phenomena such as superluminal and subluminal features [190], Doppler cloaks [185], and the Fresnel drag [190]. Spatiotemporal metamaterials offer exciting scenarios for wave interaction with unprecedented characteristics. Some of the examples include antireflection temporal coating [191], temporal aiming [192], temporal equivalent of the Brewster angle [193], temporal deflection [194], temporal asymmetry in diffusion [195], temporal twistrionics [196], and spatiotemporal waveguide cascading [197], to name a few.

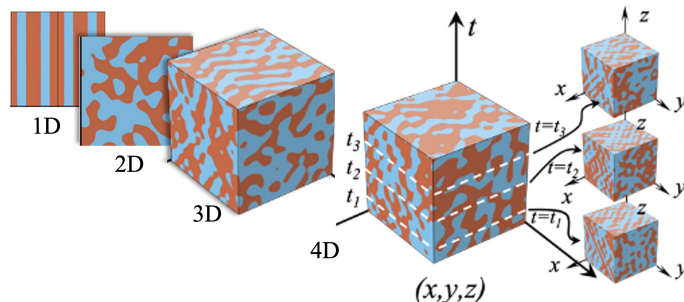


Fig. 15. One-dimensional (1D), two-dimensional (2D), three-dimensional (3D) and four-dimensional (4D) variation of parameters of material structures in electromagnetics. Adapted with permission from [198], copyright (c) American Association for the Advancement of Science. Thanks to Dr. Tzarouchis for his assistance in preparing this figure.

While adding “time” to the three dimensions of “space” can bring a larger range of functionality to metamaterials (Fig. 15) [198], one can increase even further the degrees of freedom of such platforms by properly and selectively engineering spatiotemporal variation of several components of various material parameters in order to manipulate polarization, frequency, direction of energy flow, different phase controls for different components, and other features of the waves at the same time or in particular temporal orders. For example, the temporal interface can involve temporal change an isotropic material to an anisotropic one, which may lead to phenomena such as inverse prism [199] and temporal aiming [192]. 4D metamaterials can provide new horizons for expanding the idea of transformation optics, opening doors to richer light-matter interaction. Also, perhaps in the future the 4D metamaterials can be connected to the idea of 4D imaging transient structures with electron microscopy [200]. Inspired by Kroemer’s statement about the interface, quoted above, one can envision that the temporal interface in 4D metamaterials can also provide ideas for new devices and components via hybrid combinations of spatial and temporal interfaces.

VIII. ANALOG COMPUTING USING MTS AND MTM

Metamaterials and metasurfaces can manipulate and tailor waves in unprecedented ways in order to provide unconventional functionalities. One of the interesting applications of light-matter interaction in such material platforms is wave-based analog computing. Specifically, one can explore how metastructures can be designed to function as analog computing machines with waves, providing light-speed computation

such as performing mathematical operations, vector-matrix multiplication, matrix inversion, equation solving, etc. As artificial intelligence (AI) and machine learning (ML) play increasing roles in our daily lives, it is prudent to investigate how metamaterials and metasurfaces can play important parts in data handling and signal processing, which is one of the fundamental parts of AI and ML. Optical signal processing and Fourier optics have been well-established scientific and technological fields over the past several decades [201], [202], [203], [204], [205], [206]. However, those systems are usually bulky and require proper alignment. As the field of metamaterials and metasurface has been rapidly developing with growing capability, it is natural to explore how these material media, particularly at the nanoscale, can offer exciting possibilities for wave-based, material-based analog computation. Our interest in this area started with the introduction of the notion of optical lumped circuit elements (“optical metatronics”) in 2005, [13], [207]. We asked the following question: *In the same way that in electronic and electrical circuits, we have lumped circuit elements such as inductors, capacitors, and resistors, can we have similarly lumped nanoscale circuit elements in optics, such as optical lumped nanoinductors, optical lumped nanocapacitors, and optical lumped nanoresistors?* Indeed, that became possible as we explored and presented in detail in [13] [207], where we theoretically introduced, developed, and later experimentally verified this concept using light interaction with nanostructures, [208] [209]. That idea opened up numerous possibilities in connecting the fields of electronics with photonics, allowing two-way transplantation of ideas between these two fields. One of these possible links between the two fields is in computation. We asked: *In the same way that a collection of lumped circuit elements in electronics can form an electronic circuit with specific functionality (e.g., an electronic processor, filters, etc.), can we form a collection of nanoscale lumped optical circuit elements in order to have a nanoscale photonic processor in optics?* In 2014 [88], we offered a set of recipes on how to design metamaterials that can perform mathematical operations with waves, i.e., when a monochromatic wave with an arbitrary profile enters into this material structure, the output wave would have a different profile such that the relation between the output and input profiles would be a given desired transfer function. We investigated theoretically and numerically how to design metamaterials that perform 1st- and 2nd-order spatial differentiation, spatial integration, and convolution. One of the potential applications we studied then was to explore how such metasurfaces, which performs 2nd-order differentiation, can provide edge detection. Our numerical results revealed that this is indeed possible. Following these ideas, it was later shown that nonlocalities in metasurfaces can be engineered to take advantage of the Fano resonances for achieving 1st- and 2nd-order differentiation [85], [210]. Moreover, several groups later experimentally demonstrated that it was possible to have metasurfaces that could perform edge detection [211], [212], [213], [214], [215]. Another set of applications for analog computing we explored for metasurfaces was the metamaterials that can solve equations with waves. In 2019, we introduced and developed the idea of metastructures that can

solve linear integral equations as we send an input wave into them [216]. For this application, we considered the general class of linear integral equations, i.e., the Fredholm integral equation of 2nd kind, $g(y) = I_{in}(y) + \int_a^b K(y, y')g(y')dy'$. We used the method of inverse design to design metasurfaces that can represent the generally non-separable, shift-variant kernel $K(y, y')$. We then added a feedback loop to this metasurface, which allowed the Neumann series to be performed at the speed of light (Fig. 16). Using directional couplers, we entered the input $I_{in}(y)$ into the system, while the output of the system, which is the solution of the integral equation $g(y)$, is also read using directional couplers. This was a scaled-up version in the microwave regime, providing this idea's experimental proof of concept. Later this idea was also demonstrated and verified experimentally in the optical domain using inverse-designed Si-based metagrating as optical metasurfaces, with a semi-transparent mirror as the feedback mechanism, showing capability to solve equations using free space visible radiation in a 500-nm-thick planarized metasurface platform [90]. Moreover, a single inverse-designed cylindrical nanostructure has been investigated for integral equation solving [217]. In this scenario, the inputs are in the form of an incoming wavefront illuminating this cylindrical structure, and the solution to the mathematical problem can be read in the scattered wavefront in the far zone.

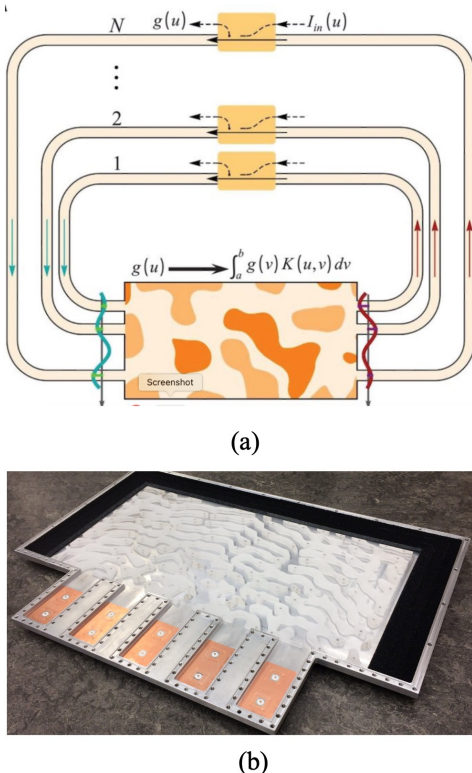


Fig. 16. Top panel) Sketch of the inverse-designed metasurface with the feedback loop and directional couplers included; (Bottom panel) the photograph of the constructed structure. Adapted with permission from [216], copyright © American Association with the Advancement of Science

One of the interesting features of optical interaction with linear media is the ability to have two waves with two dif-

ferent frequencies interacting with a single material structure without affecting each other, thus performing two different functionalities simultaneously. This property can be exploited in metasurfaces conducting near-speed-of-light, low-power parallel signal processing [218]. In [218], we numerically and experimentally demonstrated this feature in the microwave regime, showing that a single inverse-designed metastructure can solve two different linear integral equations with two different kernels $K_1(y, y')$ and $K_2(y, y')$, with arbitrary inputs $I_1(y)$ and $I_2(y)$, as the waves travel through it. In this case, the single metastructure represented the kernels $K_1(y, y')$ and $K_2(y, y')$ when the wave has the operating frequencies ω_1 and ω_2 , respectively. Most recently, we have expanded the idea of metamaterial-based analog computing into the silicon photonics platform (see Fig. 17) for vector-matrix multiplication in which we demonstrated numerically and experimentally, that 1.5-um-wavelength light propagation through a 220-nm-thick silicon slab, which is selectively etched about 70 nm in specific regions of the slab, can provide the light-speed vector-matrix multiplication.

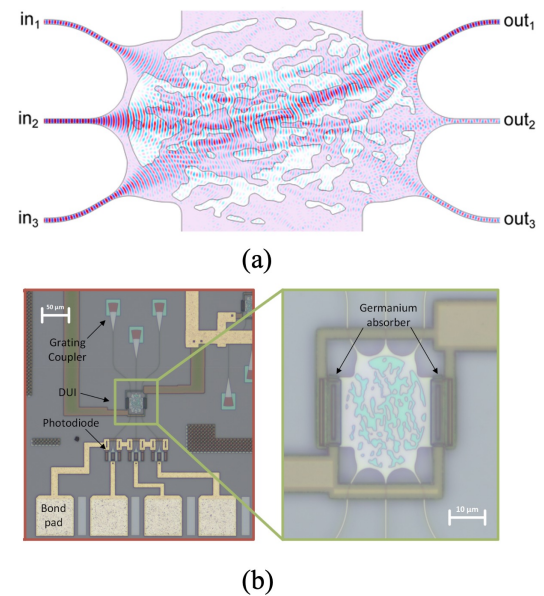


Fig. 17. Top panel) Sketch of the inverse-designed metasurface with the feedback loop and directional couplers included; (Bottom panel) the photograph of the constructed structure. Adapted with permission from [219], copyright © Springer Nature

Finally, it is important to mention that the programmability of metastructures for analog computing is highly desirable, and is currently an active area of research. We have recently demonstrated, theoretically [220] and experimentally [221], the programmability and reconfigurability of metastructures in the radio-frequency (45-MHz) domain using reconfigurable couplers in the Direct Complex Matrix (DCM) [220] architectures, showing how this system can perform matrix inversion, constraint optimization and inverse design [221]. Moreover, the use of VO₂ in reconfigurable metasurfaces for analog computing has also been recently demonstrated to enable multiple operations, switchable at fast speeds [150].

IX. CONCLUSIONS

The field of MTMs and MTSs has been thriving in the past three decades, demonstrating not only new wave phenomena defying conventional limits in electromagnetics, but also exciting applications of relevance for a wide range of technical fields, extending also beyond classical electromagnetic waves to acoustics, mechanics, quantum sciences. For metamaterials to thrive, an inherently interdisciplinary effort is necessary, which combines physics, engineering, mathematics, material science, chemistry, nanofabrication, but in which electromagnetics plays a fundamental role. In this sense, the antennas and propagation community continues to be central to this field of science and technology. One impressive aspect of metamaterials, which may be evident after reading the previous sections, is its continued evolution and timeliness. Twenty-five years ago ideas like negative-index materials and superlenses spearheaded the research in this area, but in the past decades the field has not remained stuck onto one objective, but has evolved and continues to change, open to innovations and new ideas, and involving new communities and players in the quest of advancing wave control and engineering. In this context, the antennas and propagation community continues to play a crucial role, given the degree of direct applications available and the playground offered by the microwave and mm-wave platform for experimental realization of metamaterial concepts. Many of the seminal concepts introduced in metamaterials indeed were first demonstrated, and continue to be demonstrated, at microwave frequencies in printed and integrated circuits and transmission-line devices.

Today, these concepts are becoming of key relevance in a wide range of timely applications, from the field of reconfigurable intelligent surfaces for advanced wireless networks, to analog computing and augmented reality, and even towards quantum technology applications. We forecast a continued growth of the impact of MTM and MTS technologies, as they mature into commercial products and break through new scientific domains.

REFERENCES

- [1] S. B. Glybovski, S. A. Tretyakov, P. A. Belov, Y. S. Kivshar, and C. R. Simovski, "Metasurfaces: From microwaves to visible," *Physics Reports*, vol. 634, pp. 1–72, 2016.
- [2] K. Achouri, M. A. Salem, and C. Caloz, "General metasurface synthesis based on susceptibility tensors," *IEEE Transactions on Antennas and Propagation*, vol. 63, no. 7, pp. 2977–2991, 2015.
- [3] F. Yang and Y. Rahmat-Samii, *Surface Electromagnetics, With Applications in Antenna, Microwave and Optical Engineering*. Cambridge, UK: Cambridge University Press, 2019.
- [4] A. Li, S. Singh, and D. Sievenpiper, "Metasurfaces and their applications," *Nanophotonics*, vol. 7, no. 6, pp. 989–1011, 2018.
- [5] A. Grbic and S. Maci, "Em metasurfaces [guest editorial]," *IEEE Antennas and Propagation Magazine*, vol. 64, no. 4, pp. 16–22, 2022.
- [6] T. J. Cui, A. Alù, and S. J. B. Pendry, "Guest editorial special issue on metamaterials, metadevices and applications," *IEEE Transactions on Microwave Theory and Techniques*, vol. 71, no. 8, pp. 3229–3234, 2023.
- [7] J. C. Bose, "On the rotation of plane of polarisation of electric waves by a twisted structure," *Proceedings of the Royal Society of London*, vol. 63, no. 1, pp. 146–152, 1898.
- [8] J. B. Pendry, A. J. Holden, D. J. Robbins, and W. J. Stewart, "Magnetism from conductors and enhanced nonlinear phenomena," *IEEE Transactions on Microwave Theory and Techniques*, vol. 47, no. 11, pp. 2075–2084, 1999.
- [9] J. Pendry, "Negative refraction makes a perfect lens," *Physical Review Letters*, vol. 85, no. 18, pp. 3966–3969, 2000.
- [10] R. M. Walser, "Electromagnetic metamaterials," in *Proceedings SPIE Complex Mediums II beyond Linear Isotropic Dielectrics*, 2001, pp. 1–15.
- [11] G. V. Eleftheriades and K. G. Balmain, *Negative-Refraction Metamaterials: Fundamental Principles and Applications*. John Wiley & Sons, 2005.
- [12] A. Alù and N. Engheta, "Achieving transparency with plasmonic and metamaterial coatings," *Physical Review E*, vol. 72, no. 1, p. 016623, 2005.
- [13] N. Engheta, A. Salandrino, and A. Alù, "Circuit elements at optical frequencies: Nanoinductors, nanocapacitors and nanoresistors," *Physical Review Letters*, vol. 95, no. 9, p. 095504, 2005.
- [14] J. B. Pendry, D. Schurig, and D. R. Smith, "Controlling electromagnetic fields," *Science*, vol. 312, no. 5781, pp. 1780–1782, 2006.
- [15] D. Schurig, J. J. Mock, B. J. Justice, S. A. Cummer, J. B. Pendry, A. F. Starr, and D. R. Smith, "Metamaterial electromagnetic cloak at microwave frequencies," *Science*, vol. 314, no. 5801, pp. 977–980, 2006.
- [16] Y. Ra'di and A. Alù, "Reconfigurable metagratings," *ACS Photonics*, vol. 5, no. 5, pp. 1779–1785, 2018.
- [17] A. Karvounis, B. Gholipour, K. F. Macdonald, and N. I. Zheludev, "All-dielectric phase-change reconfigurable metasurface," *Applied Physics Letters*, vol. 109, no. 5, p. 051103, 2016.
- [18] Y. Hadad, D. L. Sounas, and A. Alù, "Space-time gradient metasurfaces," *Physical Review B*, vol. 92, no. 10, p. 100304, 2015.
- [19] D. Sounas and A. Alù, "Non-reciprocal photonics based on time modulation," *Nature Photonics*, vol. 11, p. 774, 2017.
- [20] S. Hrabar, "First ten years of active metamaterial structures with 'negative' elements," *EPJ Applied Metamaterials*, vol. 5, p. 9, 2018.
- [21] N. Engheta and R. W. Ziolkowski, *Metamaterials: Physics and Engineering Exploration*. IEEE-Wiley, 2006.
- [22] R. W. Ziolkowski, "Propagation and scattering from a matched metamaterial having a zero index of refraction," *Physical Review E*, vol. 70, p. 046608, 2004.
- [23] M. Silveirinha and N. Engheta, "Tunneling of electromagnetic energy through sub-wavelength channels and bends using near-zero-epsilon materials," *Physical Review Letters*, vol. 97, p. 157403, 2006.
- [24] N. Engheta, "Pursuing near-zero response," *Science*, vol. 340, pp. 286–287, 2013.
- [25] I. Liberal and N. Engheta, "Near-zero refractive index photonics," *Nature Photonics*, vol. 11, pp. 149–158, 2017.
- [26] ———, "Zero-index platforms: Where light defies geometry," *Optics and Photonics News (OPN)*, vol. 27, pp. 28–33, 2016.
- [27] D. Vulis, O. Reshef, P. Camayd-Munoz, and E. Mazur, "Manipulating the flow of light using dirac-cone zero-index metamaterials," *Reports on Progress in Physics*, vol. 82, p. 012001, 2018.
- [28] N. Kinsey, C. DeVault, A. Boltasseva, and V. Shalaev, "Near-zero-index materials for photonics," *Nature Review Materials*, vol. 4, pp. 742–760, 2019.
- [29] M. Silveirinha and N. Engheta, "Theory of supercoupling, squeezing wave energy and field confinement in narrow channels and tight bends using epsilon-near-zero metasurfaces," *Physical Review B*, vol. 76, p. 245109, 2007.
- [30] B. Edwards, A. Alù, M. Young, M. Silveirinha, and N. Engheta, "Experimental verification of epsilon-near-zero metamaterial coupling and energy squeezing using a microwave waveguide," *Physical Review Letters*, vol. 100, p. 033903, 2008.
- [31] B. Edwards, A. Alù, M. Silveirinha, and N. Engheta, "Reflectionless sharp bends and corners in waveguides using epsilon-near-zero effects," *Journal of Applied Physics*, vol. 105, p. 044905, 2009.
- [32] J. Kim, A. Dutta, G. V. Naik, A. V. Kildishev, A. J. Giles, F. J. Bezires, C. T. Ellis, J. G. Tischler, O. J. Glembocki, A. M. Mahmoud, H. Caglayan, J. D. Caldwell, A. Boltasseva, and N. Engheta, "The role of epsilon-near-zero substrates in the optical response of plasmonic antennas," *Optica*, vol. 3, no. 3, pp. 339–346, 2016.
- [33] J.-Y. Ou, J.-K. So, G. Adamo, A. Sulava, L. Wang, and N. Zheludev, "Ultraviolet and visible range plasmonics in the topological insulator bi_{1.5}sb_{0.5}te_{1.8}se_{1.2}," *Nature Communications*, vol. 5, p. 5139, 2014.
- [34] X. Huang, Y. Lai, Z. H. Hang, H. Zheng, and C. T. Chan, "Dirac cones induced by accidental degeneracy in photonic crystals and zero-refractive-index materials," *Nature Materials*, vol. 10, pp. 582–586, 2011.
- [35] Y. Li, S. Kita, P. Munoz, O. Reshef, D. I. Vulis, M. Yin, M. Lončar, and E. Mazur, "On-chip zero-index metamaterials," *Nature Photonics*, vol. 9, no. 11, pp. 738–742, 2015.

- [36] I. Liberal, A. Mahmoud, Y. Li, B. Edwards, and N. Engheta, "Photonic doping of epsilon-near-zero media," *Science*, vol. 355, no. 6329, pp. 1058–1062, 2017.
- [37] I. Liberal, A. M. Mahmoud, and N. Engheta, "Geometry-invariant resonant cavities," *Nature Communications*, vol. 7, no. 1, pp. 1–7, 2016.
- [38] I. Liberal and N. Engheta, "Nonradiating and radiating modes excited by quantum emitters in open epsilon-near-zero (en_z) cavities," *Science Advances*, vol. 2, p. e1600987, 2016.
- [39] ———, "Zero-index structures as an alternative platform for quantum optics," *Proceedings of the National Academy of Sciences*, 2017. [Online]. Available: www.pnas.org/cgi/doi/10.1073/pnas.1611924114
- [40] A. Alù and N. Engheta, "Boosting molecular fluorescence with a plasmonic nanolauncher," *Physical Review Letters*, vol. 103, p. 043902, 2009.
- [41] A. Capretti, Y. Wang, N. Engheta, and L. D. Negro, "Enhanced third-harmonic generation in si-compatible epsilon-near-zero indium tin oxide nanolayers," *Optics Letters*, vol. 40, no. 7, pp. 1500–1503, 2015.
- [42] ———, "Comparative study of second-harmonic generation from epsilon-near-zero indium tin oxide and titanium nitride nanolayers excited in the near-infrared spectral range," *ACS Photonics*, vol. 2, pp. 1584–1591, 2015.
- [43] M. Z. Alam, I. D. Leon, and R. W. Boyd, "Large optical nonlinearity of indium tin oxide in its epsilon-near-zero regime," *Science*, vol. 352, pp. 795–797, 2016.
- [44] L. Caspani, R. P. M. Kaipurath, M. Clerici, M. Ferrera, T. Roger, J. Kim, N. Kinsey, M. Pietrzyk, A. D. Falco, V. M. Shalaev, A. Boltasseva, and D. Faccio, "Enhanced nonlinear refractive index in epsilon-near-zero materials," *Physical Review Letters*, vol. 116, p. 233901, 2016.
- [45] A. Davoyan and N. Engheta, "Theory of wave propagation in magnetized near-zero-epsilon metamaterials," *Physical Review Letters*, vol. 111, p. 257401, 2013.
- [46] A. Salandrinno and N. Engheta, "Far-field subdiffraction optical microscopy using metamaterial crystals: Theory and simulations," *Physical Review B*, vol. 74, p. 075103, 2006.
- [47] F. J. Rodríguez-Fortuño, A. Vakil, and N. Engheta, "Electric levitation using epsilon-near-zero metamaterials," *Physical Review Letters*, vol. 112, no. 3, p. 033902, 2014.
- [48] Y. Kiasat, M. G. Donato, M. Hinczewski, M. ElKabbash, T. Letsou, R. Saija, O. M. Maragò, G. Strangi, and N. Engheta, "Epsilon-near-zero (en_z)-based optomechanics," *Communications Physics*, vol. 6, p. 69, 2023.
- [49] I. Liberal and N. Engheta, "Manipulating thermal emission with spatially static fluctuating fields in arbitrarily-shaped epsilon-near-zero bodies," *Proceedings of the National Academy of Sciences*, vol. 115, pp. 2878–2883, 2018.
- [50] Y. R. R. Duggan and A. Alù, "Temporally and spatially coherent emission from thermal embedded eigenstates," *ACS Photonics*, vol. 6, pp. 2949–2956, 2019.
- [51] I. Liberal, M. Lobet, Y. Li, and N. Engheta, "Near-zero-index media as electromagnetic ideal fluids," *Proceedings of the National Academy of Sciences*, vol. 117, no. 39, pp. 24050–24054, 2020.
- [52] H. Li, Z. Zhou, W. Sun, M. Lobet, N. Engheta, I. Liberal, and Y. Li, "Direct observation of electromagnetic ideal fluids," *Nature Communications*, vol. 13, p. 4747, 2022.
- [53] C. Pfeiffer and A. Grbic, "Millimeter-wave transmitarrays for wavefront and polarization control," *IEEE Transactions on Microwave Theory and Techniques*, vol. 61, pp. 4407–4417, 2013.
- [54] N. Y. et al., "Flat optics: controlling wavefronts with optical antenna metasurfaces," *IEEE Journal of Selected Topics in Quantum Electronics*, vol. 19, p. 4700423, 2013.
- [55] A. M. H. Wong and G. V. Eleftheriades, "Perfect anomalous reflection with a bipartite huygens' metasurface," *Physical Review X*, vol. 8, p. 011036, Feb 2018.
- [56] A. Epstein and G. V. Eleftheriades, "Arbitrary power-conserving field transformations with passive lossless omega-type bianisotropic metasurfaces," *IEEE Transactions on Antennas and Propagation*, vol. 64, no. 9, pp. 3880–3895, 2016.
- [57] G. Atalaglou, M. Chen, M. Kim, and G. V. Eleftheriades, "Microwave huygens' metasurfaces: Fundamentals and applications," *IEEE Journal of Microwaves*, vol. 1, no. 1, pp. 374–388, Winter 2021.
- [58] N. Yu, P. Genevet, M. A. Kats, F. Aieta, J.-P. Tetienne, F. Capasso, and Z. Gaburro, "Light propagation with phase discontinuities: generalized laws of reflection and refraction," *Science*, vol. 334, no. 6054, pp. 333–337, 2011.
- [59] X. Ni, N. K. Emani, A. V. Kildishev, A. Boltasseva, and V. M. Shalaev, "Broadband light bending with plasmonic nanoantennas," *Science*, vol. 335, no. 6067, p. 427, 2012.
- [60] Ra'di and S. A. Tretyakov, "Balanced and optimal bianisotropic particles: maximizing power extracted from electromagnetic fields," *New Journal of Physics*, vol. 15, p. 053008, 2013.
- [61] T. Niemi, A. O. Karilainen, and S. A. Tretyakov, "Synthesis of polarization transformers," *IEEE Transactions on Antennas and Propagation*, vol. 61, no. 6, pp. 3102–3111, 2013.
- [62] J. Budhu and A. Grbic, "Recent advances in bianisotropic boundary conditions: theory, capabilities, realizations and applications," *Nanophotonics*, vol. 10, no. 16, pp. 4075–4112, 2021.
- [63] C. Pfeiffer and A. Grbic, "Bianisotropic metasurfaces for optimal polarization control: Analysis and synthesis," *Physical Review Applied*, vol. 2, p. 044011, 2014.
- [64] A. Epstein and G. V. Eleftheriades, "Arbitrary power-conserving field transformations with passive lossless omega-type bianisotropic metasurfaces," *IEEE Transactions on Antennas and Propagation*, vol. 64, no. 9, pp. 3880–3895, Sep 2016.
- [65] F. Giusti, E. Martini, S. Maci, and M. Albani, "Comparison between different approaches for the design of anomalous refractors," *IEEE Transactions on Antennas and Propagation*, vol. 72, no. 4, pp. 3495–3506, 2024.
- [66] A. Benini, E. Martini, S. Monni, M. C. Viganò, F. Silvestri, E. Gandini, G. Gerini, G. Toso, and S. Maci, "Phase-gradient meta-dome for increasing grating-lobe-free scan range in phased arrays," *IEEE Transactions on Antennas and Propagation*, vol. 66, no. 8, pp. 3973–3982, 2018.
- [67] A. Monti, S. Vellucci, M. Barbuto, D. Ramaccia, and F. Bilotti, "Quadratic-gradient metasurface-dome for wide-angle beam-steering phased array with reduced gain loss at broadside," *IEEE Transactions on Antennas and Propagation*, vol. 71, no. 2, pp. 2022–2027, 2023.
- [68] A. Díaz-Rubio et al., "Achromatic metalenses: Broadband focusing using refractive index gradients," *ACS Photonics*, vol. 8, no. 5, pp. 1286–1293, 2021.
- [69] D. Sell et al., "Large-angle, multifunctional metagratings based on freeform multimode geometries," *IEEE Transactions on Antennas and Propagation*, vol. 62, no. 11, pp. 5780–5791, 2014.
- [70] S. Pancharatnam, "Generalized theory of interference and its applications," *Proceedings of the Indian Academy of Sciences, Section A*, vol. 44, no. 5, pp. 247–262, 1956.
- [71] M. V. Berry, "Quantal phase factors accompanying adiabatic changes," *Proceedings of the Royal Society of London. Series A, Mathematical and Physical Sciences*, vol. 392, no. 1802, pp. 45–57, 1984.
- [72] Y.-H. L. et al., "Recent progress in pancharatnam–berry phase optical elements and the applications for virtual/augmented realities," *Optical Data Processing and Storage*, vol. 3, no. 1, pp. 79–88, 2017.
- [73] V. Sozio, E. Martini, F. Caminita, P. D. Vita, M. Faenzi, A. Giacomini, M. Sabbadini, S. Maci, and G. Vecchi, "Design and realization of a low cross-polarization conical horn with thin metasurface walls," *IEEE Transactions on Antennas and Propagation*, vol. 68, no. 5, pp. 3477–3486, 2020.
- [74] M. J. Mencagli, E. Martini, S. Maci, and M. Albani, "A physical optics approach to the analysis of metascreens," *IEEE Access*, vol. 8, pp. 162634–162641, 2020.
- [75] M. D. R. et al., "Smart radio environments empowered by reconfigurable intelligent surfaces: How it works, state of research and the road ahead," *IEEE Journal on Selected Areas in Communications*, vol. 38, no. 11, pp. 2450–2525, 2020.
- [76] ———, "Smart radio environments empowered by reconfigurable ai meta-surfaces: An idea whose time has come," *EURASIP Journal on Wireless Communications and Networking*, vol. 2019, p. 129, 2019.
- [77] P. Y. Chen and S. A. Tretyakov, "A three-layer intelligent metasurface structure for routing control signals," *Physical Review Applied*, vol. 11, no. 4, p. 044024, 2019.
- [78] L. Zhou et al., "Programmable metasurfaces with multi-layer architecture for control signal routing," *Advanced Optical Materials*, vol. 8, no. 12, p. 2000783, 2020.
- [79] F. Monticone, N. M. Estakhri, and A. Alù, "Full control of nanoscale optical transmission with a composite metascreen," *Physical Review Letters*, vol. 110, p. 203903, 2013.
- [80] Y. Radi, D. Sounas, and A. Alù, "Meta-gratings: beyond the limits of graded metasurfaces for wavefront control," *Physical Review Letters*, vol. 119, p. 067404, 2017.
- [81] Y. Radi and A. Alù, "Metagratings for efficient wavefront manipulation," *IEEE Photonics Journal*, vol. 14, p. 2207513, 2022.

- [82] A. Overvig and A. Alù, "Diffractive nonlocal metasurfaces," *Laser and Photonics Reviews*, vol. 16, p. 2100633, 2022.
- [83] ——, "Wavefront-selective fano resonant metasurfaces," *Advanced Photonics*, vol. 3, p. 026002, 2021.
- [84] S. C. Malek, A. C. Overvig, A. Alù, and N. Yu, "Multifunctional resonant wavefront-shaping meta-optics based on multilayer and multi-perturbation nonlocal metasurfaces," *Light*, vol. 11, p. 246, 2022.
- [85] H. Kwon, D. Sounas, A. Cordaro, A. Polman, and A. Alù, "Nonlocal metasurfaces for optical signal processing," *Physical Review Letters*, vol. 121, p. 173004, 2018.
- [86] Y. Zhou, H. Zheng, I. I. Kravchenko, and J. Valentine, "Flat optics for image differentiation," *Nature Photonics*, vol. 14, p. 316, 2020.
- [87] M. Cotrufo, A. Arora, S. Singh, and A. Alù, "Dispersion engineered metasurfaces for broadband, high-na, high-efficiency, dual-polarization analog image processing," *Nature Communications*, vol. 14, p. 7078, 2023.
- [88] A. Silva, F. Monticone, G. Castaldi, V. Galdi, A. Alù, and N. Engheta, "Performing mathematical operations with metamaterials," *Science*, vol. 343, no. 6167, pp. 160–163, January 2014.
- [89] H. Zheng, Q. Liu, I. I. Kravchenko, X. Zhang, Y. Huo, and J. G. Valentine, "Multichannel meta-imagers for accelerating machine vision," *Nature Nanotechnology*, 2024, in press.
- [90] A. Cordaro, B. Edwards, V. Nikkhah, A. Alù, N. Engheta, and A. Polman, "Solving integral equations in free-space with inverse-designed ultrathin optical metagratings," *Nature Nanotechnology*, vol. 18, p. 365, 2023.
- [91] A. Overvig, S. A. Mann, and A. Alù, "Thermal metasurfaces: complete emission control by combining local and nonlocal light-matter interactions," *Physical Review X*, vol. 11, p. 021050, 2021.
- [92] P. P. Iyer, R. A. DeCrescent, Y. Mohtashami, G. Lheureux, N. A. Butakov, A. Alhassan, C. Weisbuch, S. Nakamura, S. P. DenBaars, and J. A. Schuller, "Unidirectional luminescence from ingan/gan quantum-well metasurfaces," *Nature Photonics*, vol. 14, p. 543, 2020.
- [93] G. W. Hanson, "Dyadic green's functions and guided surface waves for a surface conductivity model of graphene," *IEEE Transactions on Antennas and Propagation*, vol. 59, no. 10, pp. 3448–3459, 2011.
- [94] A. Alù and N. Engheta, "Effect of nonlocality on guided wave propagation and plasmonic response of thin graphene slabs," *Science*, vol. 337, no. 6093, pp. 1140–1144, 2012.
- [95] A. Vakil and N. Engheta, "Transformation optics using graphene," *Science*, vol. 332, no. 6035, pp. 1291–1294, 2011.
- [96] A. B. Yakovlev and G. W. Hanson, "Spectral and modal properties of open waveguide structures formed by grounded uniaxial slabs," *IEEE Transactions on Antennas and Propagation*, vol. 57, no. 1, pp. 78–89, 2009.
- [97] S. Maci, G. Minatti, M. Casaletti, and M. Bosiljevac, "Metasurfing: Addressing waves on impenetrable metasurfaces," *IEEE Antennas and Wireless Propagation Letters*, vol. 10, pp. 1499–1502, 2011.
- [98] R. Quarfoth and D. Sievenpiper, "Artificial tensor impedance surface waveguides," *IEEE Transactions on Antennas and Propagation*, vol. 61, no. 7, pp. 3597–3606, July 2013.
- [99] ——, "Surface wave scattering reduction using beam shifters," *IEEE Antennas and Wireless Propagation Letters*, vol. 13, pp. 963–966, 2014.
- [100] G. Minatti, M. Faenzi, E. Martini, F. Caminita, P. D. Vita, D. González-Ovejero, M. Sabbadini, and S. Maci, "Modulated metasurface antennas for space: Synthesis, analysis and realizations," *IEEE Transactions on Antennas and Propagation*, vol. 63, no. 4, pp. 1288–1300, Apr. 2015.
- [101] B. H. Fong, J. S. Colburn, J. J. Ottusch, J. L. Visher, and D. F. Sievenpiper, "Scalar and tensor holographic artificial impedance surfaces," *IEEE Transactions on Antennas and Propagation*, vol. 58, no. 10, pp. 3212–3221, 2010.
- [102] D. González-Ovejero, N. Chahat, R. Sauleau, G. Chattopadhyay, S. Maci, and M. Ettorre, "Additive manufactured metal-only modulated metasurface antennas," *IEEE Transactions on Antennas and Propagation*, vol. 66, no. 11, pp. 6106–6114, Nov 2018.
- [103] M. Faenzi, G. Minatti, D. González-Ovejero, F. Caminita, E. Martini, C. D. Giovampaola, and S. Maci, "Metasurface antennas: New models, applications and realizations," *Scientific Reports*, vol. 9, no. 1, July 2019.
- [104] G. Minatti, F. Caminita, E. Martini, and S. Maci, "Flat optics for leaky-waves on modulated metasurfaces: Adiabatic floquet-wave analysis," *IEEE Transactions on Antennas and Propagation*, vol. 64, no. 9, pp. 3896–3906, Sept 2016.
- [105] G. Minatti, F. Caminita, E. Martini, M. Sabbadini, and S. Maci, "Synthesis of modulated-metasurface antennas with amplitude, phase and polarization control," *IEEE Transactions on Antennas and Propagation*, vol. 64, no. 9, pp. 3907–3919, Sept 2016.
- [106] G. Xu, A. Overvig, and Y. K. et al., "Arbitrary aperture synthesis with nonlocal leaky-wave metasurface antennas," *Nature Communications*, vol. 14, p. 4380, 2023.
- [107] D. González-Ovejero and S. Maci, "Gaussian ring basis functions for the analysis of modulated metasurface antennas," *IEEE Transactions on Antennas and Propagation*, vol. 63, no. 9, pp. 3982–3993, Sept 2015.
- [108] S. Maci and A. Cucini, "Fss-based ebg surface," in *Electromagnetic Metamaterials: Physics and Engineering Aspects*, N. Engheta and R. Ziolkowski, Eds. Hoboken, NJ: Wiley, 2006.
- [109] M. A. Francavilla, E. Martini, S. Maci, and G. Vecchi, "On the numerical simulation of metasurfaces with impedance boundary condition integral equations," *IEEE Transactions on Antennas and Propagation*, vol. 63, no. 5, pp. 2153–2161, May 2015.
- [110] A. Oliner and A. Hessel, "Guided waves on sinusoidally-modulated reactance surfaces," *IRE Transactions on Antennas and Propagation*, vol. 7, no. 5, pp. 201–208, December 1959.
- [111] E. Martini, F. Caminita, and S. Maci, "Double-scale homogenized impedance models for periodically modulated metasurfaces," *EPJ Applied Metamaterials*, vol. 7, p. 12, 2020.
- [112] M. Faenzi, D. González-Ovejero, and S. Maci, "Flat gain broadband metasurface antennas," *IEEE Transactions on Antennas and Propagation*, vol. 69, no. 4, pp. 1942–1951, April 2021.
- [113] G. Minatti, M. Faenzi, M. Sabbadini, and S. Maci, "Bandwidth of gain in metasurface antennas," *IEEE Transactions on Antennas and Propagation*, vol. 65, no. 6, pp. 2836–2842, June 2017.
- [114] G. Minatti, E. Martini, and S. Maci, "Efficiency of metasurface antennas," *IEEE Transactions on Antennas and Propagation*, vol. 65, no. 4, pp. 1532–1541, April 2017.
- [115] J. S. Gomez-Diaz, M. Tymchenko, and A. Alù, "Hyperbolic metasurfaces: surface plasmons, light-matter interactions and physical implementation using graphene strips [invited]," *Optical Materials Express*, vol. 5, no. 10, p. 2313, 2015.
- [116] A. A. H. et al., "Visible-frequency hyperbolic metasurface," *Nature*, vol. 522, no. 7555, pp. 192–196, 2015.
- [117] C. L. Cortes and Z. Jacob, "Super-coulombic atom-atom interactions in hyperbolic media," *Nature Communications*, vol. 8, no. 1, p. 14144, 2017.
- [118] Z. Guo, H. Jiang, Y. Li, H. Chen, and G. S. Agarwal, "Enhancement of electromagnetically induced transparency in metamaterials using long range coupling mediated by a hyperbolic material," *Optics Express*, vol. 26, no. 2, p. 627, 2018.
- [119] G. Palermo, K. V. Sreekanth, N. Maccaferri, G. E. Lio, G. Nicoletta, F. D. Angelis, M. Hinczewski, and G. Strangi, "Hyperbolic dispersion metasurfaces for molecular biosensing," *Nanophotonics*, 2020.
- [120] A. N. Poddubny, P. A. Belov, P. Ginzburg, A. V. Zayats, and Y. S. Kivshar, "Microscopic model of purcell enhancement in hyperbolic metamaterials," *Physical Review B*, vol. 86, no. 3, 2012.
- [121] A. Poddubny, I. Iorsh, P. Belov, and Y. Kivshar, "Hyperbolic metamaterials," *Nature Photonics*, vol. 7, no. 12, pp. 948–957, 2013.
- [122] C. A. Valagiannopoulos, M. S. Mirmoosa, I. S. Nefedov, S. A. Tretyakov, and C. R. Simovski, "Hyperbolic-metamaterial antennas for broadband enhancement of dipole emission to free space," *Journal of Applied Physics*, vol. 116, no. 16, p. 163106, 2014.
- [123] B. Li, Y. He, and S. He, "Investigation of light trapping effect in hyperbolic metamaterial slow-light waveguides," *Applied Physics Express*, vol. 8, no. 8, p. 082601, 2015.
- [124] T. Zhumabek and C. Valagiannopoulos, "Light trapping by arbitrarily thin cavities," *Physical Review Research*, vol. 2, no. 4, p. 043349, 2020.
- [125] A. V. Chshelokova, P. V. Kapitanova, A. N. Poddubny, D. S. Filonov, A. P. Slobozhanyuk, P. A. Belov, and Y. S. Kivshar, "Hyperbolic transmission-line metamaterials," *Journal of Applied Physics*, vol. 112, no. 7, p. 073116, 2012.
- [126] C. L. Cortes, W. Newman, S. Molesky, and Z. Jacob, "Quantum nanophotonics using hyperbolic metamaterials," *Nature Photonics*, vol. 7, pp. 287–293, 2012.
- [127] A. Benini, A. M. Barrera, E. Martini, A. Toccafondi, and S. Maci, "Self-complementary hyperbolic metasurface antennas," *IEEE Transactions on Antennas and Propagation*, vol. 71, no. 5, pp. 3816–3827, 2023.
- [128] S. Yves, E. Galiffi, X. Ni, E. M. Renzi, and A. Alù, "Twist-induced hyperbolic shear metasurfaces," *Physical Review X*, vol. 14, no. 2, p. 021031, 2024.
- [129] E. M. Renzi, E. Galiffi, X. Ni, and A. Alù, "Hyperbolic shear metasurfaces," *Physical Review Letters*, vol. 132, no. 26, p. 263803, 2024.

- [130] O. Yermakov, V. Lenets, A. Sayanskiy, J. D. Baena, E. Martini, S. B. Glybovski, and S. Maci, "Surface waves on self-complementary metasurfaces: All-frequency hyperbolicity, extreme canalization and tetm polarization degeneracy," *Physical Review X*, vol. 11, no. 3, p. 031038, 2021.
- [131] D. González-Ovejero, G. Minatti, G. Chattopadhyay, and S. Maci, "Multibeam by metasurface antennas," *IEEE Transactions on Antennas and Propagation*, vol. 65, no. 6, pp. 2923–2930, 2017.
- [132] Y. Wen, P. Y. Qin, S. Maci, and Y. J. Guo, "Low-profile multibeam antenna based on modulated metasurface," *IEEE Transactions on Antennas and Propagation*, vol. 71, no. 8, pp. 6568–6578, 2023.
- [133] M. Faenzi, D. González-Ovejero, G. Petraglia, G. D'Alterio, F. Pascale, R. Vitiello, and S. Maci, "A metasurface radar monopulse antenna," *IEEE Transactions on Antennas and Propagation*, vol. 70, no. 4, pp. 2571–2579, 2021.
- [134] Y. Ge, K. P. Esselle, and T. S. Bird, "The use of simple thin partially reflective surfaces with positive reflection phase gradients to design wideband, low-profile ebg resonator antennas," *IEEE Transactions on Antennas and Propagation*, vol. 60, no. 2, pp. 743–750, 2012.
- [135] J. Ruiz-García, E. Martini, C. D. Giovampaola, D. González-Ovejero, and S. Maci, "Reflecting luneburg lenses," *IEEE Transactions on Antennas and Propagation*, vol. 69, no. 7, pp. 3924–3935, Jul. 2021.
- [136] C. Bilitos, X. Morvan, E. Martini, R. Sauleau, S. Maci, and D. González-Ovejero, "Broadband reflecting luneburg lenses based on bed-of-nails metasurfaces," *IEEE Transactions on Antennas and Propagation*, vol. 72, no. 2, pp. 1923–1928, Feb. 2024.
- [137] C. Bilitos, X. Morvan, R. Sauleau, E. Martini, S. Maci, and D. González-Ovejero, "Series dual-fed continuous transverse stub array with enhanced multibeam operation enabled by a reflective luneburg lens," *IEEE Transactions on Antennas and Propagation*, vol. 72, no. 11, pp. 8420–8432, Nov. 2024.
- [138] F. Liu *et al.*, "Intelligent metasurfaces with continuously tunable local surface impedance for multiple reconfigurable functions," *Physical Review Applied*, vol. 11, p. 044024, Apr. 2019.
- [139] K. Chen, Y. Feng, F. Monticone, J. Zhao, B. Zhu, T. Jiang, L. Zhang, Y. Kim, X. Ding, S. Zhang, A. Alù, and C.-W. Qiu, "A reconfigurable active huygens' metalens," *Advanced Materials*, vol. 29, no. 17, p. 1606422, 2017.
- [140] S. C. Pavone, E. Martini, F. Caminita, M. Albani, and S. Maci, "Surface wave dispersion for a tunable grounded liquid crystal substrate without and with metasurface on top," *IEEE Transactions on Antennas and Propagation*, vol. 65, no. 7, pp. 3540–3548, 2017.
- [141] C. Della Giovampaola, F. Caminita, G. Labate, E. Martini, and S. Maci, "Experimental verification of a 5g active metasurface antenna with beam steering capabilities," in *2021 15th European Conference on Antennas and Propagation (EuCAP)*, 2021.
- [142] C. Caloz, A. Alù, S. Tretyakov, D. Sounas, K. Achouri, and Z.-L. Deck-Léger, "Electromagnetic nonreciprocity," *Physical Review Applied*, vol. 10, no. 4, p. 047001, 2018.
- [143] K. Fang, Z. Yu, and S. Fan, "Realizing effective magnetic field for photons by controlling the phase of dynamic modulation," *Nature Photonics*, vol. 6, pp. 782–787, 2012.
- [144] D. L. Sounas, C. Caloz, and A. Alù, "Giant non-reciprocity at the subwavelength scale using angular momentum-biased metamaterials," *Nature Communications*, vol. 4, pp. 1–7, 2013.
- [145] N. A. Estep, D. L. Sounas, J. Soric, and A. Alù, "Magnetic-free nonreciprocity and isolation based on parametrically modulated coupled-resonator loops," *Nature Physics*, vol. 10, pp. 923–927, 2014.
- [146] F. Ruesink, M.-A. Miri, A. Alù, and E. Verhagen, "Nonreciprocity and magnetic-free isolation based on optomechanical interactions," *Nature Communications*, vol. 7, pp. 1–8, 2016.
- [147] Z. Yu and S. Fan, "Complete optical isolation created by indirect interband photonic transitions," *Nature Photonics*, vol. 3, pp. 91–94, 2009.
- [148] S. Fan *et al.*, "Nonreciprocal photonics based on time modulation," *Science*, vol. 364, p. eaat3100, 2019.
- [149] H. Lira, Z. Yu, S. Fan, and M. Lipson, "Electrically driven nonreciprocity induced by interband photonic transition on a silicon chip," *Physical Review Letters*, vol. 109, p. 033901, 2012.
- [150] M. Cotrufo, A. Cordaro, D. L. Sounas, A. Polman, and A. Alù, "Passive bias-free non-reciprocal metasurfaces based on thermally nonlinear quasi-bound states in the continuum," *Nature Photonics*, vol. 18, no. 1, pp. 81–90, 2024.
- [151] D. L. Sounas and A. Alù, "Fundamental bounds on the operation of fano nonlinear isolators," *Physical Review B*, vol. 97, no. 11, p. 115431, 2018.
- [152] Y. Radi, N. Nefedkin, P. Popovski, and A. Alù, "Nonlinear, active and time-varying metasurfaces for wireless communications: A perspective and opportunities," *IEEE Antennas and Propagation Magazine*, vol. 66, no. 5, pp. 52–62, October 2024.
- [153] T. Ozawa, H. M. Price, A. Amo, N. Goldman, M. Hafezi, L. Lu, M. C. Rechtsman, D. Schuster, J. Simon, O. Zilberberg, and I. Carusotto, "Topological photonics," *Reviews of Modern Physics*, vol. 91, no. 1, p. 015006, 2019.
- [154] A. Slobobzhanuk, A. V. Shchelokova, X. Ni, S. H. Mousavi, D. A. Smirnova, P. A. Belov, A. Alù, Y. S. Kivshar, and A. B. Khanikaev, "Near-field imaging of spin-locked edge states in an all-dielectric topological metasurface," *Applied Physics Letters*, vol. 114, no. 3, p. 031103, January 2019.
- [155] A. Khanikaev and A. Alù, "One-way photons in silicon," *Nature Photonics*, vol. 8, pp. 680–682, September 2014.
- [156] M. G. Silveirinha, "Topological classification of chern-type insulators by means of the photonic green function," *Phys. Rev. X*, vol. 4, p. 031054, 2014.
- [157] Q. Song, M. Odeh, J. Zúñiga-Pérez, B. Kanté, and P. Genevet, "Plasmonic topological metasurface by encircling an exceptional point," *Science*, vol. 373, no. 6559, pp. 1133–1137, 2021.
- [158] Z. Sakotić, A. Krasnok, A. Alù, and N. Janković, "Topological scattering singularities and embedded eigenstates for polarization control and sensing applications," *Photonics Research*, vol. 9, no. 7, pp. 1310–1323, 2021.
- [159] A. Krasnok, D. Baranov, H. Li, M. A. Miri, F. Monticone, and A. Alù, "Anomalies in light scattering," *Advances in Optics and Photonics*, vol. 11, no. 4, pp. 892–951, 2019.
- [160] M. A. Miri and A. Alù, "Exceptional points in optics and photonics," *Science*, vol. 363, no. 6422, p. eaar7709, 2019.
- [161] R. Kolkowski, S. Kovács, and A. F. Koenderink, "Plasmonic topological metasurface by encircling an exceptional point," *Physical Review Research*, vol. 3, no. 2, p. 023185, 2021.
- [162] M. G. Silveirinha, "Ptd symmetry-protected scattering anomaly in optics," *Physical Review B*, vol. 95, no. 3, p. 035153, 2017.
- [163] E. Martini, M. G. Silveirinha, and S. Maci, "Exact solution for the protected tem edge mode in a ptd-symmetric parallel-plate waveguide," *IEEE Transactions on Antennas and Propagation*, vol. 67, no. 2, pp. 1035–1044, November 2018.
- [164] X. M. Mitsallas, C. De Angelis, and S. Maci, "Exact solution of a ptd-symmetric bifilar-line waveguide formed by parallel-plate impedance junctions," *IEEE Transactions on Antennas and Propagation*, vol. 72, no. 10, pp. 7830–7840, 2024.
- [165] I. Nadeem, V. Verri, E. Martini, F. Morgia, A. Toccafondi, M. Mattivi, and S. Maci, "Experimental verification of backscattering protection in ptd-symmetric bifilar edge waveguides," *IEEE Transactions on Antennas and Propagation*, vol. 70, no. 11, pp. 10632–10640, 2022.
- [166] I. Nadeem, E. Martini, A. Toccafondi, and S. Maci, "Flexible unidirectional ptd-symmetric waveguide," *Radio Science Letters*, vol. 3, no. 1, pp. 282–289, 2021.
- [167] I. Nadeem, V. Verri, E. Martini, F. Morgia, M. Mattivi, A. Toccafondi, and S. Maci, "Switchable edge-line coupler based on parity time-reversal duality symmetry," *Scientific Reports*, vol. 12, no. 1, p. 19011, 2022.
- [168] I. Nadeem, N. Castro, E. Martini, A. Toccafondi, E. Rajo-Iglesias, and S. Maci, "Backscattering protection in a fully metallic ptd-symmetric bifilar edge line (bel)," *IEEE Transactions on Antennas and Propagation*, vol. 72, no. 8, pp. 6807–6812, 2024.
- [169] S. Singh, R. J. Davis, D. J. Bisharat, J. Lee, S. M. Kandil, E. Wen, X. Yang, Y. Zhou, P. R. Bandaru, and D. F. Sievenpiper, "Advances in metasurfaces: Topology, chirality, patterning and time modulation," *IEEE Antennas and Propagation Magazine*, vol. 64, no. 4, pp. 51–62, 2022.
- [170] N. Mohammadi Estakhri, N. Engheta, and R. Kastner, "Electromagnetic funnel: Reflectionless transmission and guiding of waves through subwavelength apertures," *Physical Review Letters*, vol. 124, no. 3, p. 033901, 2020.
- [171] H. Kroemer, "Quasi-electric fields and band offset," in *Nobel Lecture in Physics*, 2000, presented in Stockholm, Sweden, December 8, 2000. [Online]. Available: <https://www.nobelprize.org/prizes/physics/2000/kroemer/lecture/>
- [172] L. A. Zadeh, "The determination of the impulsive response of variable networks," *Journal of Applied Physics*, vol. 21, no. 6, pp. 642–645, 1950.
- [173] ———, "Frequency analysis of variable networks," *Proceedings of the IRE*, vol. 38, no. 3, pp. 291–299, 1950.

- [174] F. Morgenthaler, "Velocity modulation of electromagnetic waves," *IRE Transactions on Microwave Theory and Techniques*, vol. 6, no. 2, pp. 167–172, 1958.
- [175] R. L. Fante, "Transmission of electromagnetic waves into time-varying media," *IEEE Transactions on Antennas and Propagation*, vol. 19, no. 3, pp. 417–424, 1971.
- [176] E. Galiffi, R. Tirole, S. Yin, H. Li, S. Vezzoli, P. A. Huidobro, M. G. Silveirinha, R. Sapienza, A. Alù, and J. B. Pendry, "Photonics of time-varying media," *Advanced Photonics*, vol. 4, no. 1, p. 014002, 2022.
- [177] S. Yin and A. Alù, "Efficient phase conjugation in a spacetime leaky waveguide," *ACS Photonics*, vol. 9, no. 3, pp. 979–985, 2022.
- [178] M. Lyubarov, Y. Lumer, A. Dikopoltsev, E. Lustig, Y. Sharabi, and M. Segev, "Amplified emission and lasing in photonic time crystals," *Science*, vol. 377, no. 6606, pp. 425–428, 2022.
- [179] F. Biancalana, A. Amann, A. V. Uskov, and E. P. O'Reilly, "Dynamics of light propagation in spatiotemporal dielectric structures," *Physical Review E*, vol. 75, no. 4, p. 046607, 2007.
- [180] J. R. Zurita-Sánchez, P. Halevi, and J. C. Cervantes-González, "Reflection and transmission of a wave incident on a slab with a time-periodic dielectric function," *Physical Review A*, vol. 79, no. 5, p. 053821, 2009.
- [181] E. Lustig, Y. Sharabi, and M. Segev, "Topological aspects of photonic time crystals," *Optica*, vol. 5, no. 11, pp. 1390–1395, 2018.
- [182] G. Ptitsyn, M. S. Mirmoosa, and S. A. Tretyakov, "Time-modulated meta-atoms," *Physical Review Research*, vol. 1, no. 2, p. 023014, 2019.
- [183] S. Vezzoli, V. Bruno, C. DeVault, T. Roger, V. M. Shalaev, A. Boltasseva, M. Ferrera, M. Clerici, A. Dubietis, and D. Faccio, "Optical time reversal from time-dependent epsilon-near-zero media," *Physical Review Letters*, vol. 120, p. 043902, 2018.
- [184] T. T. Koutserimpas and R. Fleury, "Nonreciprocal gain in non-hermitian time-floquet systems," *Physical Review Letters*, vol. 120, p. 087401, 2018.
- [185] D. Ramaccia, D. L. Sounas, A. Alù, A. Toscano, and F. Bilotti, "Doppler cloak restores invisibility to objects in relativistic motion," *Physical Review B*, vol. 95, p. 075113, 2017.
- [186] ——, "Phase-induced frequency conversion and doppler effect with time-modulated metasurfaces," *IEEE Transactions on Antennas and Propagation*, vol. 68, p. 1607, 2019.
- [187] V. Bacot, M. Labousse, A. Eddi, M. Fink, and E. Fort, "Time reversal and holography with spacetime transformations," *Nature Physics*, vol. 12, p. 972, 2016.
- [188] H. Moussa, G. Xu, S. Yin, E. Galiffi, Y. Radi, and A. Alù, "Observation of temporal reflection and broadband frequency translation at photonic time interfaces," *Nature Physics*, vol. 19, p. 863–868, 2023.
- [189] D. L. Sounas and A. Alù, "Angular-momentum-biased nanorings to realize magnetic-free integrated optical isolation," *ACS Photonics*, vol. 1, p. 198, 2014.
- [190] P. A. Huidobro, E. Galiffi, S. Guenneau, R. V. Craster, and J. Pendry, "Fresnel drag in space-time-modulated metamaterials," *Proceedings of the National Academy of Sciences*, vol. 116, p. 24943, 2019.
- [191] V. Pacheco-Pena and N. Engheta, "Antireflection temporal coatings," *Optica*, vol. 7, p. 323, 2020.
- [192] ——, "Temporal aiming," *Light: Science Applications*, vol. 9, p. 129, 2020.
- [193] ——, "Temporal equivalent of brewster angle," *Physical Review B*, vol. 104, p. 214308, 2021.
- [194] ——, "Spatiotemporal isotropic-to-anisotropic meta-atoms," *New Journal of Physics*, vol. 23, p. 095006, 2021, special issue on "Focus on Active Metamaterials and Metasurfaces".
- [195] M. Camacho, B. Edwards, and N. Engheta, "Achieving asymmetry and trapping in diffusion with spatiotemporal metamaterials," *Nature Communications*, vol. 11, p. 3733, 2020.
- [196] G. Ptitsyn and N. Engheta, "Temporal twistrionics," *ArXiv*, 2024, arXiv:2403.10477, submitted under review.
- [197] V. Pacheco-Pena and N. Engheta, "Spatiotemporal cascading of dielectric waveguides," *Optical Materials Express*, vol. 14, no. 4, pp. 1062–1073, 2024, feature issue on "Time-varying artificial photonic metastructures".
- [198] N. Engheta, "Four-dimensional optics using time-varying metamaterials," *Science*, vol. 379, p. 1190, 2023.
- [199] A. Akbarzadeh, N. Chamanara, and C. Caloz, "Inverse prism based on temporal discontinuity and spatial dispersion," *Optics Letters*, vol. 43, p. 3297, 2018.
- [200] B. Barwick, H. S. Park, O.-H. Kwon, J. S. Baskin, and A. H. Zewail, "4d imaging of transient structures and morphologies in ultrafast electron microscopy," *Science*, vol. 322, p. 1227, 2008.
- [201] W. Rotman and R. Turner, "Wide-angle microwave lens for line source applications," *IEEE Transactions on Antennas and Propagation*, vol. 11, no. 6, pp. 623–632, 1963.
- [202] S. K. Yao and S. H. Lee, "Spatial differentiation and integration by coherent optical-correlation method," *Journal of the Optical Society of America*, vol. 61, pp. 474–477, 1971.
- [203] S. H. Lee, "Optical analog solutions of partial differential and integral equations," *Optical Engineering*, vol. 24, no. 1, p. 240141, 1985.
- [204] H. Rajbenbach, Y. Fainman, and S. H. Lee, "Optical implementation of an iterative algorithm for matrix inversion," *Applied Optics*, vol. 26, pp. 1024–1031, 1987.
- [205] J. W. Goodman, *Introduction to Fourier Optics*. New York: McGraw-Hill, 1968.
- [206] M. Ferrera, Y. Park, L. Razzari, B. E. Little, S. T. Chu, R. Morandotti, D. J. Moss, and J. Azeña, "On-chip cmos-compatible all-optical integrator," *Nature Communications*, vol. 1, p. 29, 2010.
- [207] N. Engheta, "Circuits with light at nanoscales: Optical nanocircuits inspired by metamaterials," *Science*, vol. 317, pp. 1698–1702, 2007.
- [208] Y. Sun, B. Edwards, A. Alù, and N. Engheta, "Experimental realization of optical lumped nanocircuit elements at infrared wavelengths," *Nature Materials*, vol. 11, pp. 208–212, March 2012.
- [209] H. Caglayan, S.-H. Hong, B. Edwards, C. Kagan, and N. Engheta, "Near-ir metatronic nanocircuits by design," *Physical Review Letters*, vol. 111, p. 073904, August 2013, (5 pages).
- [210] H. Kwon, A. Cordaro, D. Sounas, A. Polman, and A. Alù, "Dual-polarization analog 2d image processing with nonlocal metasurfaces," *ACS Photonics*, vol. 7, pp. 1799–1805, 2020.
- [211] A. Cordaro, H. Kwon, D. Sounas, A. F. Koenderink, A. Alù, and A. Polman, "High-index dielectric metasurfaces performing mathematical operations," *Nano Letters*, vol. 19, p. 8418–8423, 2019.
- [212] Y. Zhou, H. Zheng, I. I. Kravchenko, and J. Valentine, "Flat optics for image differentiation," *Nature Photonics*, vol. 14, pp. 316–323, 2020.
- [213] A. Pors, M. G. Nielsen, and S. I. Bozhevolnyi, "Analog computing using reflective plasmonic metasurfaces," *Nano Letters*, vol. 15, no. 1, pp. 791–797, 2015.
- [214] T. Zhu, Y. Zhou, Y. Lou, H. Ye, M. Qiu, Z. Ruan, and S. Fan, "Plasmonic computing of spatial differentiation," *Nature Communications*, vol. 8, p. 15391, 2017.
- [215] C. Guo, M. Xiao, M. Minkov, Y. Shi, and S. Fan, "Photonic crystal slab laplace operator for image differentiation," *Optica*, vol. 5, no. 3, pp. 251–256, 2018.
- [216] N. M. Estakhri, B. Edwards, and N. Engheta, "Inverse-designed metasurfaces that solve equations," *Science*, vol. 363, no. 6433, pp. 1333–1338, March 22 2019.
- [217] H. Goh and A. Alù, "Nonlocal scatterers for compact wave-based analog computing," *Physical Review Letters*, vol. 128, p. 073201, 2022.
- [218] M. Camacho, B. Edwards, and N. Engheta, "A single inverse-designed photonic structure that performs parallel computing," *Nature Communications*, vol. 12, p. 1466, 2021.
- [219] V. Nikkhah, A. Pirmoradi, F. Ashtiani, B. Edwards, F. Aflatouni, and N. Engheta, "Inverse-designed low-index-contrast structures on silicon photonics platform for vector-matrix multiplication," *Nature Photonics*, vol. 18, pp. 501–508, May 2024.
- [220] D. Tzarouchis, M. J. Mencagli, B. Edwards, and N. Engheta, "Mathematical operations and equation solving with reconfigurable metadevices," *Light Science and Applications*, vol. 11, p. 263, 2022.
- [221] D. Tzarouchis, B. Edwards, and N. Engheta, "Programmable wave-based analog computing machines: A metastructure that designs metasurfaces," *Nature Communications*, vol. 16, p. 908, January 2025.